

IDENTIFICATION AND MODELING OF INTERNAL WAVES

TECHNICAL REPORT No.
NIO/TR-02/2007

T.V.Ramana Murty
Y.Sadhuram
M.M.Malleswara Rao
S.Sujith Kumar
K.Maneesha
K.Sai Sandhya
S.Surya Prakash
P.Chandramouli
K.S.R.Murthy



2007



NATIONAL INSTITUTE OF OCEANOGRAPHY
DONA PAULA, GOA-403004, INDIA

Contents

- Contributors to the project
- List of Tables
- List of Figures
- Summary

- 1. Introduction
 - 1.1 Details of data collection
- 2. Results
 - 2.1 Variability of temperature, salinity, density, Brunt vaiala frequency and sound velocity under different seasons
 - 2.2 Currents
 - 2.3 Identification of Internal Waves
 - 2.4 Characterstics of Internal waves from CTD and Spectrum analysis
 - 2.5 Internal wave field generation
 - 2.6 Modelling of Internal waves
 - 2.7 Internal wave simulation
- 3. Conclusion

Contributors to the project

- | | |
|--------------------------|-----------------|
| 1. Dr.T.V.Ramana Murty | Co-investigator |
| 2. Dr.Y.Sadhuram | Member |
| 3. Dr.M.M.Malleswara Rao | Member |
| 4. Mr.S.Sujith Kumar | Member |
| 5. Mr.S.Surya Prakash | Member |
| 6. Mr.P.Chandramouli | Member |

Others

7. Miss K.Maneesha
8. Miss K.Sai Sandhya

List of Tables:

- Table 1:** Details of data collection
- Table 2:** Internal Wave model run
- Table 3:** Internal wave characteristics off Visakhapatnam during Sep 2005
Internal wave velocity (c) – 0.029 km/hr
- Table 4:** Internal wave characteristics off Bhimili during Feb 2007
Internal wave velocity (c) – 0.042 km/hr
- Table 5:** Internal wave characteristics off KG Basin
- Table 6:** Acoustic Propogational Characteristics
- Table 7:** Acoustic Ray parameters - January 2005
- Table 8:** Acoustic Ray parameters - September 2005
- Table 9:** Acoustic Ray parameters - October 2006
- Table 10:** Acoustic Ray parameters - February 2007

List of figures and Plates:

- Fig 1** Cruise track of sasu-84 and the fixed location for time-series data on currents and CTD
- Fig 2** Time series data on Temperature ($^{\circ}\text{C}$) off Visakhapatnam (VSP) ($17^{\circ}23.7'\text{N}$, $83^{\circ}28.5'\text{E}$) and Bhimili ($17^{\circ}35.486'\text{N}$, $83^{\circ}42.322'\text{E}$)
- Fig 3** Time series data on Salinity (psu) off Visakhapatnam (VSP) ($17^{\circ}23.7'\text{N}$, $83^{\circ}28.5'\text{E}$) and Bhimili ($17^{\circ}35.486'\text{N}$, $83^{\circ}42.322'\text{E}$)
- Fig 4** Time series data on Density (kg/m^3) off Visakhapatnam (VSP) ($17^{\circ}23.7'\text{N}$, $83^{\circ}28.5'\text{E}$) and Bhimili ($17^{\circ}35.486'\text{N}$, $83^{\circ}42.322'\text{E}$)
- Fig 5** Variation of Brunt Visalia's frequency (cph) off Visakhapatnam (VSP) ($17^{\circ}23.7'\text{N}$, $83^{\circ}28.5'\text{E}$) and Bhimili ($17^{\circ}35.486'\text{N}$, $83^{\circ}42.322'\text{E}$)
- Fig 6** Variation of Sound velocity (m/sec) off Visakhapatnam (VSP) ($17^{\circ}23.7'\text{N}$, $83^{\circ}28.5'\text{E}$) and Bhimili ($17^{\circ}35.486'\text{N}$, $83^{\circ}42.322'\text{E}$)
- Fig 7** Mean vertical distribution of a) Temperature ($^{\circ}\text{C}$) b) Salinity (psu) c) Density (kg / m^3) d) Sound velocity (m/sec) e) Brunt-viasala's Frequency (cph) off Visakhapatnam during 4 January, 18 September 2005 and 18 October 2006.
- Fig 8 (a)** Time series data on (a) Temperature ($^{\circ}\text{C}$) (b) Direction ($^{\circ}\text{c}$) Speed (m/sec)(d) U-component (m/sec) (e) V-component (m/sec) at 10m depth off Visakhapatnam (VSP)
- Fig 8 (b)** Time series data on (a) Temperature ($^{\circ}\text{C}$) (b) Direction ($^{\circ}\text{c}$) Speed (m/sec) (d) U-component (m/sec) (e) V-component (m/sec) at 60m depth off Visakhapatnam (VSP)

Fig 8 (c) Time series data on (a) Temperature ($^{\circ}\text{C}$) (b) Direction ($^{\circ}$) (c) Speed (m/sec) (d) U-component (m/sec) (e) V-component (m/sec) at 10m depth off Visakhapatnam (VSP)

Fig 8 (d) Time series data on (a) Temperature ($^{\circ}\text{C}$) (b) Direction ($^{\circ}$) (c) Speed (m/sec) (d) U-component (m/sec) (e) V-component (m/sec) at 60m depth off Visakhapatnam (VSP)

Fig 9 (a) Time series data on temperature (2 minute) collected from Thermister chain at off Visakhapatnam during 18-20 Oct2006

Fig 9 (b) Time series data on temperatures (2 minute) collected from thermister chain at off Bhimili during 23-25 Feb2007

Fig 10 (a) Energy density spectra of temperature oscillations at a) 10m and b) 60m off Visakhapatnam (vsp) during 4/1/05 to 6/1/05

Fig 10 (b) Energy density spectra of temperature oscillations at a) 10m and b) 60m off Visakhapatnam (vsp) during 18/9/05

Fig 10 (c) Energy spectra of temperature oscillations at depths 5m, 10m, 25m, 50m, 75m, 100m off Visakhapatnam (vsp) during 18-20 Oct 2006

Fig 10 (d) Energy spectra of temperature oscillations at depths 5m, 10m, 25m, 50m, 75m, 100m off Bhimili (vsp) during 23-25 Feb2007

Fig 11 (a) Internal wave modes for frequencies (cph) (a) 8 (b) 7.99 (c) 7.98 (d) 7.97 Off Visakhapatnam during January 2005

Fig 11 (b) Internal wave modes for frequencies (cph) (a) 1.5 (b) 1.49 (c) 1.48 (d) 1.47 off Visakhapatnam during September 2005

Fig 11 (c) Internal wave modes for frequencies (cph) (a) 1.5 (b) 1.49 (c) 1.48 (d) 1.47 Off Visakhapatnam during October 2006

Fig 11 (d) Internal wave modes for frequencies (cph) (a) 8 (b) 7.99 (c) 7.98 (d) 7.97 off Visakhapatnam during February 2007

Fig 12. Internal wave dispersion relations

Fig 13 Sound velocity relations (a- single b-double) in 50 min ,10min apart off VSP and Bhimili

Fig 14 Sound velocity relations (a-single-double) in 9 km, 0.1 km apart off VSP & Bhimili

Fig 15 Temporal dependence of sound velocity distribution in the internal wave field (single & double realizations) off VSP & Bhimili

Fig 16 Spatial dependence of sound velocity distribution in the internal Wave field (Single & double realizations) off VSP & Bhimili

Fig 17 Ray paths

Fig 18 Transmission loss by Kracken model

Fig 19 Transmission loss in 3-D form

Plates 1 and 2 Preparations for time-series data collection using CTD, Current Meters and thermister chain

Summary

Naval Research Board (NRB), New Delhi, sanctioned a collaborative project among I.I.T., New Delhi, N.I.O. Regional Centre Visakhapatnam and Dept. of Meteorology and Oceanography, Andhra University(AU), Visakhapatnam in the month of November 2003. The main aim of this project is Identification and modeling of Internal Waves off Visakhapatnam and Bhimili coast with an ultimate goal to help the naval operations.

N.I.O. Regional Centre, had planned systematic field experiments under different seasons (winter, monsoon, post-monsoon, late winter) to meet the objectives of the project. The results based on the above experiments are compared with the satellite imageries (AU) and model outputs (IIT). There is a good agreement between the observed and model results. Overall results of the project during 2003-2007 are presented in the final report. The present report results are based on insitu observations and acoustic model simulation studies carried out by NIO, RC, Visakhapatnam.

Abstract:

Analyses of Internal Wave (IW) signatures by insitu observations off Visakhapatnam have been presented to study the impact of IWs on acoustic field. Temperature data were collected for 44 hours off Visakhapatnam ($17^{\circ}26.46'N$ and $83^{\circ}31.20'E$) and Bhimili ($17^{\circ}35.486'N$, $83^{\circ}42.322'E$) at sonic depth 100 m during different seasons using time series CTD (hourly), current meter and indigenously developed thermister chain (at an interval of 2 minutes) to study the Internal Wave (IW) characteristics. Sound velocity realizations (in space and time) in the observed High Frequency (HF) IW field is generated utilizing Garret-Munk (GM) model. Acoustic propagation simulation is carried out in the IW HF field over 9 km (cycles) needed for navy objectives for different source-receiver configurations with cutoff frequency through field observations. Transmission loss anomaly with reference to mean are found to be 3-9 dB for normal conditions while 30 dB in disturbed conditions.

1. Introduction:

Naval Research Board (NRB), New Delhi sanctioned a collaborative project to I.I.T., New Delhi ; NIO, Regional Center Visakhapatnam and Department of Meteorology and Oceanography, Andhra University, Visakhapatnam in the month of Nov 2003. The main objective of this project is to develop numerical model for generation and propagation of Internal Waves (IW) through field measurements and satellite imageries. The NIO, RC component of the main objective is as follows

- Study of Acoustic propagation and fluctuations with reference to internal waves off Visakhapatnam and surrounding waters from observed data.
- Normal mode modeling to calculate:
 - i) Propagation anomaly loss
 - ii) Absorption Loss
 - iii) Total loss with different frequencies and ranges using field data

Relevant data to identify the internal waves off Visakhapatnam coast had been collected under different seasons. The data had been collected on board our research vessel CRV Sagar Sukti and mechanized boats. The details of data collection are shown in Table.1

Table.1 Details of data collection

	period	Details of data collection
1 st Phase	4 - 10 Jan 2005	CTD and currents
2 nd phase	18 - 19 Sep 2005	CTD, currents and Thermistor chain
3 rd phase	18 - 20 Oct 2006	CTD, and Thermistor chain
4 th phase	23-25 Feb 2007	CTD, and Thermistor chain

1.1 Details of Data collection

1st Phase:

A cruise on board CRV Sagar Sukthi had been planned to collect time series CTD data at a fixed location ($17^{\circ} 23.7'N$, $83^{\circ} 28.5'E$) off Visakhapatnam and along the transects off Visakhapatnam coast during 4th to 10th January, 2005, a few days after the Sumatra Tsunami which devastated the east coast of India on 26th December, 2004. Simultaneously, time series data on currents at the same location for 48 hours (4th to 6th January, 2005) at 90 m water depth were collected by deploying two RCM-7 Current Meters (Aanderaa Instruments, Norway) at 10 m and 60 m water depths. The time interval was fixed at 2 minutes and the current meter was deployed at 60 m which lies in the thermocline region, to identify the internal waves in winter season. CTD data was collected using SBE19 plus Seacat Profiler (Seabird Electronics, USA).

The cruise track and the location for time series measurements as detailed in Table 1 are shown in Fig.1. Since the data was collected after few days of the tsunami, the effect of the incident on 26th December 2004 at Visakhapatnam harbour is briefly mentioned here.

“According to the fishermen the water level within the fishing harbour raised approximately 3.0 m above mean sea level (msl) around 09.30 hrs and flooded the fishing harbour premises. The travelers and boats in the harbour moved without any control. Within about 10 minutes the water level reached the record lower level of 2.5 m below msl. About 1 m wall of water gushed into the harbour and raised the level to 2.5 m. Similar raise and fall of water levels were observed till 11.30 hrs. The tide gauge recorded a maximum level of 2.3 m at 09.25 hrs and reached minimum level of 2.7 below msl at 11.30 hrs with intervening seven fluctuations at 10 to 15 minutes intervals. The tidal wave again reached a maximum level of 2.05 m at 12.00 hrs and minimum level of 2.9m (above msl) at 12.15 hrs. (Gaitan Vaz, 2005). Since this coincided with the time of high tide, the excess water due to tsunami resulted in flooding of the fishing harbour. There was no abnormal variation in the waterline at Ramakrishna Beach. It seems that the water level receded by 100 m at Bhogapuram (20 km north of Visakhapatnam). According to port authorities the maximum current during this event was about 5 knots in the inner harbour area. There were no damages and loss of life at Visakhapatnam.” The impact of the tsunami on coastal waters was reported earlier (Sadhuram et.al, 2007).

2nd Phase

Data collection for the monsoon season had been planned from 18th – 20th, September 2005, at the same location (data collected in earlier season) keeping in view of the satellite passes over the study area during the above period.

Demonstration of Thermister chain is also planned along with this fieldwork programme. Thermister chain with 5 sensors to record temperature at 5 depths (5 m, 25 m, 50 m, 75 m and 100 m) was operated to obtain the time series data at 2 minute interval. The data had been collected on 17th and 18th September (Plates 1&2). Unfortunately, the data collection was disturbed by a depression, which formed in the head Bay of Bengal on 17th September. It intensified into a deep depression and moved in southwesterly direction, which was quite abnormal and crossed Kalingapatnam on 19th September 2005. In view of the safety of the personnel and equipment, the fieldwork program had been abandoned on 18th night after collecting data for a few hours.

3rd Phase

Data collection during post-monsoon season was planned during 18-20 October 2006 at 100m depth off Visakhapatnam on board a mechanized boat. Time series CTD data (hourly interval) and temperature data (at 2 minute interval at 5 depths as described above) had been collected continuously. Unfortunately, the data on currents could not be obtained as the rotors were lost after deployment due to strong currents. Most of the CTD profiles could not go to deeper depth as the instrument drifted heavily due to strong currents. Thermistor chain worked well and we could get good data for all the five depths.

4th Phase:

After examining the satellite imageries it is found that occurrence of internal waves is quite dominant off Bhimili. Hence, we have planned to collect time series data off Bhimili during 23-25 Feb 2007 (late winter) and accordingly collected at 100m sonic depth(17^o35.486'N 83^o42.322'E). Weather was favourable and sea was calm and so both CTD and thermistor chain data recording is quite good.

Progress of the project work had been presented before the NRB committee for every 6 months and the progress reports were submitted. Overall results of the project during 2003-2007 have been presented in this final report.

2. Results

2.1. Variability of temperature, salinity, density, Brunt Vaisala Frequency and sound velocity under different seasons

Temperature: During winter, strong inversions of 2°C are seen at 40-50 m depth. Temperature at surface was about 26°C increased to 28°C at middle depth and further decreased with the depth. Though inversions are common off Visakhapatnam during winter, it appears that they are some what stronger (Fig.2a). Temperature in the surface layer is > 29°C and at 50 m it was around 26°C during monsoon season (Fig.2b) while it was about 30°C in the top layer during post monsoon season . The data could not be recorded below 30m depth as the instrument drifted heavily. It was around 29°C in the 20-30 m layer. (Fig.2c). During late winter, the top layer (up to 50 m) is dominated by 27°C isotherm with mild inversions. Strong oscillations are observed between 60-90 m depth indicating the presence of internal waves. The temperature at the bottom is about 21°C (Fig.2d).

Salinity: Salinity was 27-28 psu at surface and around 35 psu at bottom that shows a strong vertical gradient. Strong oscillations are seen in the mid depth during winter. Large gradients could be seen in salinity, which was 29 and 34 psu at surface and 50 m respectively. It was around 30 psu in the top layer during monsoon season (Figs.3a&b). Low salinities (22-24 psu) were observed in the top (5 m) layer and it was about 29 psu at 50 m depth that shows strong gradients in the salinity structure under post monsoon season. This could be mainly due to the transport of low saline waters from North Bay towards south by the East India Coastal current. During late winter, there is not much variation in

the salinity from top to bottom (32 to 35 psu). (Fig.3d). Surface density was low (1017 kg/m^3) on the first day and increased to 1019 kg/m^3 on the next day. One could notice a strong oscillation in the density structure on the first day compared with the second day. The impact of salinity could be seen in the density structure. The top layer is dominated by low density (1010 kg/m^3) during post-monsoon and high density 1021 kg/m^3 during late winter (Fig.4).

Maximum values (30-60 cph) of Brunt Vaisala Frequency (N^2) were observed in the top layer during post-monsoon which indicates strong stratification followed by monsoon season. High values (10-20 cph) are observed in the middle layer during the other seasons.(Fig.5 and Table2) . Very strong gradients are observed in the sound velocity in the top and bottom layers during post-monsoon and late winter seasons respectively. In general it varied from 1539-1541 m/sec in the mid depths during all the seasons (Fig.6).

Mean profiles (of temperature, salinity, density, sound velocity and Brunt Viasala's Frequency) under different seasons are shown in Fig.7. One can see large variations in the profiles between the seasons. An increase of about 3°C in temperature and a decrease of about 4 psu in salinity could be seen from winter to monsoon season. Similarly, there is an increase in sound velocity and N^2 . Highest value (30 cph) of N^2 was observed at 10 m depth. Sound velocity was about 1530 m/sec during winter increased to 1541 m/sec by monsoon season. During post-monsoon season, sound velocity varied from 1535 m/sec (surface) to 1512 m/sec (bottom). Strong variations with season could be seen in the top 20 m layer in case of N^2 .

2.2 Currents

Time series data on speed (m/sec) and direction of current at 10 m and 60 m depths collected during winter season are shown in the Figs.8a & b. Temperature, U and V components of the currents are also plotted. Temperature

at 10 m depth is fluctuating around 26 - 26.5°C in the beginning and showed a sudden drop of 1°C on the next day, and was fluctuating around 25.5°C. Speed of current was 0.40-0.60 m/sec with direction 220⁰-240⁰ (south ward), almost parallel to the coast. Meridional component (V) is stronger (-0.30 to -0.60 m/sec) than the zonal (u) component (-0.2 to -0.4 m/sec). Temperature at 60 m depth mostly varied between 23-24°C. Flow is southwest with a speed of 0.4-0.6 m/sec. It appears that there is not much gradient in the current speed between 10 m and 60 m. U and V at 60m components also are similar to that observed at 10 m. This suggests that the flow is strong and consistent throughout the layer up to 60 m depth during the observational period .Time series data (2 min interval) on currents at 10 m and 60 m depths under monsoon season, are shown in Figs 8c&d. This data was collected when the depression was intensifying and moving in a Southwesterly direction, which is quite abnormal. Strong currents >0.8 m/sec were recorded during the observational period. The direction was highly fluctuating because of the influence of the depression. Both U and V components are also stronger. Temperature (at 10 m depth) was fluctuating between 28 and 29°C. At 60 m depth, speed was 0.3-0.4 m/sec while the direction was mostly between 220-230°.

2.3 Identification of Internal waves

Time series data on temperature at five depths (5m, 25m, 50m 75m and 100m) at 2 minute interval obtained from the Thermistor chain during monsoon (18 Sept., 2005) , Post-monsoon (18-20 October 2006) and late winter (23-25 Feb, 2007) are shown in Fig. 9. The temperature data collected at 10 m and 60 m depths by two RCM-7 current meters during winter and post-monsoon seasons are also used for the computations.

These data were Fast Fourier Transformed (FFT) to examine the spectral characteristics of the temperature oscillations in the study area off Visakhapatnam and Bhimili (Mahadevan et.al., 1987). The power spectra of

temperature fluctuations at 7 vertical depths (5m,10m,25m,50m,60m,75m,100m) were computed to study the short period internal waves with one ensemble and 3 ensemble data sets and are presented in Fig.10. The FFT results reveal that the frequencies of waves are found to vary between 0.1 -1.2 cph which comes under small scale statistical component (i.e. random with respect to the acoustic time scale). This frequency range represents small scale fluctuations caused by internal waves and also microstructures. The Internal Waves(IW) can be categorized as combinations of low (< 0.5 cph) and high (> 0.5 cph) frequencies. The spectral energy estimates of IW are higher in deeper depths compared to shallow (Figs.10 a-d).The IW spectral energy in the thermocline is the highest in the entire water column as compared to other depths(above and below). This phenomenon may be due to high stratification of water column. It is interesting to see that internal waves off Bhimili during late winter appear to be generated by the bottom forces. This is possible when a quasi steady current advects in a stratified ocean, bottom topography generates standing internal waves known as “lee waves” (Garret and Munk 1979). Even though IW are propagating in the stratified waters off Bhimili over bottom topography (during Feb, 2006), relatively higher spectral energy is not seen at this depth. This loss of energy as compared to other depths may be due to bottom boundary layer, which acted as energy sink rather than energy source (Garett and Munk, 1979). However off Visakhapatnam internal waves were observed in the thermocline region due to stratification which is in contrast to the above feature. As these small scale fluctuations in the temperature due to IW are comparable to acoustic wave scales, the results of present analysis may be utilized in acoustic transmission experiments for detection of under water objects (utilizing appropriate acoustic models). From the above analysis we derived the following IW characteristics of dominant frequencies and their periods off Visakhapatnam and Bhimili Tables (3 to 5).

Frequencies- Upper limit of IW band is from 17-23 cph in calm conditions while in disturbed conditions it is 34.24 cph. Dominant high frequency of IW

field is observed between 0.02-0.40cph(LF) while it is 0.7 - 8.0 cph for HF.

Periods : Overall time periods of IW field vary between 2.5 - 40.0 hrs (LF) while for HF 0.127-1.33 hrs

2.4 Characteristics of Internal Waves from CTD and spectrum analysis:

IW characteristics are computed based on CTD mean profiles of time-series and IW periods obtained from spectrum analysis. The following equation has been adopted for computation of IW wavelength (Antony et.al 1985; Murty and Murty, 1986)

$$\text{Wave length } L = c T \dots\dots\dots(1)$$

where speed of the internal wave c , is given by

$$c^2 = \frac{gh_1h_2}{h_1 + h_2} \left(\frac{\rho + \rho'}{\rho} \right)$$

h_1 = thickness of the top layer of weak density gradient

h_2 =thickness of the bottom layer of strong density gradient

ρ = mean density of top layer

ρ' =mean density of bottom layer

g = acceleration due to gravity

T = IW period (from frequency analysis)

The IW characteristics off Visakhapatnam, Bhimili and K-G basin are presented in Tables 3-5 for LF and HF

Speeds : Average IW speed is 0.035 km/hr

Wave length: Overall average wave lengths are varying between 0.07-2.1km(LF) while for HF 0.005 - 0.009 km. These LF band of IW wave lengths

are comparable with satellite images(away from the shore) whereas HF of IW band are not confirmed by those images due to limitations in resolving small features nearer to coast.

2.5 Internal wave field generation:

Physical variability occurs in the ocean with space (scales of millimeters to planetary) and time (from seconds to geological times) due to external and internal forcing (Robinson and Ding Lee, 1994). Physical oceanographers are interested to study variability of ocean environment rather than its mean. Oceanic changes relevant to underwater acoustics are classified into mean and fluctuating components (De Santo's 1979) with the following general model of the sound speed equation

$$C(r, t) = C_0(z) + \delta C_1(r) + \delta c_2(r, t) \quad (2)$$

z – depth, t -time, r - three-dimensional position

having characteristics: 1) a mean vertical profile $C_0(z)$ that represents local climatology($C_0 \sim 1500$ m/s), 2) a meso scale component($\delta C_1(r)$) (fronts, eddies) -- deterministic with respect to the acoustic time scale ($\delta C_1/C_0 \sim 10^{-2}$), and 3) a statistical component ($\delta c_2(r, t)$) (i.e random with respect to the acoustic time scale, $\delta C_2/C_0 \sim 10^{-4}$) that represents small scale fluctuations caused by Internal Waves (IW) and fine and microstructure. The IW frequencies extend from inertial frequency. The IW of semidiurnal frequency –internal tides- dominate the low frequency (LF) band of IW, while IW of >0.5 cph dominate the high frequency(HF) band of IW.

2.6 Modeling of Internal Waves

The IW parameters vary with space and time. Their measurements at sea are too expensive. Therefore successful modeling of IW provides the IW parameters at any interested site in the sea. Garret and Munk (GM) (1975)

succeeded in modeling deep water IW-GM model – and later improved it for shallow water IW, (Munk , 1981). This GM model requires time-series data on temperature field for frequency analysis and CTD data for stratification parameter Brunt-vaisala frequency. More details on IW modeling for generation of HF IW field are given by Krishna Kumar & Balasubramanian (2005).

2.7 Internal wave simulation:

Internal wave simulation has been carried out for identification and prediction of high-frequency internal waves with space and time utilizing the time series CTD, currents and thermister chain data. Internal wave eigen-frequencies and modes (Fig. 11a-d) at a specified sequence of horizontal wave numbers are computed using “finite difference – Sturm sequence – bisection – inverse iteration method”, with mean profiles (Fig. 7 & 12). From these modal calculations, sequences of sound speed realizations (Figs 13-16) are obtained using the Garrett-Munk internal wave spectrum model (Table 2, Fig. 12)). Using temporal (Fig. 13) and spatial distribution (Fig. 14) of sound speed realizations, the range-independent and range-dependent numerical ray tracing and Kraken model experiments have been conducted to obtain eigen rays (Fig. 17) and transmission losses (Figs. 18-19) etc., to study the impact of internal waves on sound propagation.

The Buoyancy Frequency profile was generated using the collected temperature and salinity profiles on uniform mesh, with a depth increment of $\Delta z = 2$ m for the purpose of computing the internal wave modes and eigen-frequencies (Fig.10). In the present model, care is taken to see that the local Brunt-Vaisala Frequency is between 0.024cph (inertial frequency) to 34.24cph (maximum frequency) (Table 2) and stratification scale ($B=1.3$ km) (Ramana Murty et.al,1989).

A wave number sampling increment of $\Delta k = 0.01$ cycles/km was used with samples between 0.5 cycles/km (lower bound of HF) and higher bound of HF to compute normal modes (Table 2). A total of 40 internal wave modes and eigen-frequencies were computed at each of the above 20 positive wave numbers as

specified in Table 2. The dispersion relations between the wave number and eigen-frequencies are plotted and shown in Fig.12. Energy density factor of $E_0 = 4$ was used to generate realizations of displacements. Sound velocity profiles (C) were obtained by adding the fluctuations (δC_2) in the following equation (Munk and Zachariassen, 1976) to the background profile (C_0)

$$\delta C_2(r, z, t) \cong (dc_p / dz) \text{Re}[\zeta(r, z, t)] \text{---(3)}$$

where dc_p / dz is the potential sound velocity gradient (m/sec) and $\zeta(r, z, t)$ the internal wave displacement function.

Sound velocity profiles were generated for every 600 sec (10 minutes) between 0 and 3000 sec (50 minutes) and every 0.1 km between the range 0 and 9 km. The temporal dependence of the sound velocity is shown in Fig.13 for a single and double realization of the internal wave field (Flatte', et.al, 1979). The spatial dependence is shown in Fig. 14. The temporal and spatial distribution in the internal wave fields are presented in the contour forms (Figs.15 & 16). The range dependence of the sound velocity profile is the most important consequence of the internal waves, on the temporal and spatial scales selected.

The spatial - independence (Without Internal Waves-WIW) spatial - dependence(IW) of sound velocity profiles have been used as input (in Fig 14 & left panel of Fig. 17) to trace the rays between source-receiver configuration at specified depths (Table 6), to compute eigen rays (middle panel of Fig. 17) and their corresponding intensity losses (right panel of Fig. 17 and Figs 18-19). The corresponding ray parameters history is shown in Tables 7-10 for the rang of 9 km (over 9 cycles).

The columnwise ray nomenclature in Tables 7-10 are detailed as a footnote. The columns 5 to 10 of Table 7-10 explains number of upper (p^+) and lower (p^-) ray turnings, number of top (p_t^+) and bottom (p_b^-) ray bonks, and overall total number of ray turnings (p^+)₊(p^-) and bonks [(p_t^+) + (p_b^-)] This information can be used as ray identifier. The ray identifier enables us to identify

the rays from their arrival patterns, since the rays usually arrive at the receiver end in groups. There are four classes of rays 1) R/R (purely refracted both above and beneath the axis, $p_t^+ = p_b^- = 0$) 2) SR/R (surface reflected and refracted, $p_t^+ \neq 0, p_b^- = 0$), 3) R/BR (refracted and bottom reflected, $p_t^+ = 0, p_b^- \neq 0$) and 4) SR/BR (surface and bottom reflected, $p_t^+ \neq 0, p_b^- \neq 0$). From Tables (7-10) one can conclude only the SR/R category rays are seen among all possible above classes. The travel times are clustered, may be due to the anticipated ray path degeneracy (Munk and Wunsch, 1979) (Table 7-10). To avoid ray path degeneracy, in the present simulation experiment, cumulative intensity loss (Moler & Soloman, 1970) also been computed in the presence of IW and without IW (Table 6) considering the phase shift with sub-surface-duct frequency (Urlick, 1975) instead of individual ray paths. The anomaly explains the impact of IW on acoustic propagation characteristics in HF IW field. From Table - 6, one can conclude that the transmission loss anomaly with reference to mean are found to be 3 - 9 dB for normal conditions while 30dB in disturbed conditions. The Transmission loss by Kraken model (Porter and Reiss, 1984, Porter 1992) of normal mode theory also computed and it is indicated that there is 10 dB loss over the range of 9 km in HF IW field. Finally we have simulated 3-D transmission loss of stratified waters, off Visakhapatnam using canonical sound velocity model by WKBZ mode approach (Zhang et.al, 1993) and presented in the Fig.19 (Munk and Wunsch, 1979). Fig.19 explains the total loss with different frequencies, ranges and depths and can be used as template for naval operations at sea.

3. Conclusions

1. Internal Wave (IW) Characteristics Based on Field Measurements-

Frequencies- Upper limit of IW band from 17-23 cph in calm conditions while in disturbed conditions it is 34.24 cph. Dominant high frequency of IW field is observed between 0.02-0.40cph (LF) while it is 0.7 -8.0 cph for HF

Periods: Overall time periods of IW field vary between 2.5 - 40.0 hr (LF) while for HF 0.127-1.33 hrs

Speeds : Average IW speed is 0.035 km/hr

Wave length: Overall Average wave lengths are varying between 0.07-2.1km (LF) while for HF 0.005-0.009 km

2. Acoustic Propagation Characteristics:

Acoustic propagation simulation is carried out in high frequency IW field over 9 km (9 cycles) for different source receiver configurations with cutoff acoustic frequency through field observation .Transmission loss anomaly with reference to mean are found to be 3-9 dB for normal conditions while 30 dB in disturbed conditions.

Acknowledgements:

We thank NRB, New Delhi for funding this project and Dr. D. Srinivasan, and Sri K.R.G.K.Murthy former Heads, OEP of NRB and Dr.R.R.Rao, Scientist-G, NPOL Cochin, for their constant support and constructive and valuable suggestions through out this project (GAP-1434). We are also thankful to Dr.S.R.Shetye, Director, NIO and Drs. A.D.Rao, IIT New Delhi; K.V.S.R.Prasad, AU others investigators of NRB collaborative project. Thanks

are also due to Sri Sreejith, of M/s EMCON, Kochi, for his pains taking efforts in field participations to test supplied thermistor chain field worthiness.

References:

[1] Gaitan Vaz .G, 2005: Tsunami news on “An eyewitness account from Visakhapatnam” Jour.Geol.Soc.India, Vol 65 pp 139-140

[2] Sadhuram.Y, Murty.T.V.R., and Rao B.P., 2007: Hydrophysical manifestation of the Indian Ocean Tsunami, Chapter in a book on “ The Indian Ocean Tsunami” eds: Tad Murty, U.Aswathanarayana and N. Nirupama , Taylor and Francis Group London , U.K., pp 365-372.

[3] Mahadevan R, Swaminathan . T, and Issac Martin M, 1987: ” Ocean surface wave analysis”, TR.No. 27, Ocean Engineering center I.I.T. Madras pp. 115

[4] Garrett. C, and Munk .W., 1979: Internal Waves in the Ocean, Ann. Rev. Fluid Mech. 11: pp 339-369

[5]Antony M.K., Murty C.S., Reddy G.V., and Rao K.H., 1985: Estuarine, Coastal and shelf science, 21 pp 823-834.

[6] Murthy P .G. K and G. R.K Murthy, 1986:, “A case study on the influence of internal waves on sound propagation in the sea ”, Journal of Sound and Vibration, 108 (3), 447

[7] Robinson. Allan.R. and Lee D., 1994 : “Oceanography and Acoustics” AIP press. American Institute of Physics, Woodbury, NY, 11797-2999 ,p 256

[8] Desanto J.A., “Theoretical Methods in Ocean Acoustics”, in Ocean Acoustics edited by Desanto J.A., (Springer-Verlag, New York, 1979) pp 7-77; see also Dugan J.P., Oceanography in Under water Acoustics Chapter 5.

[9] Garret C.J., and Munk .W., 1975: “ Space-time scales of internal waves: Aprogress report”, J. Geophy. Res., 80, pp 291-297

[10] Munk. W. 1981: “ In evolution of Physical Oceanography”, MIT press, Massachusetts, USA.

[11] Krishna Kumar G.V., and Balasubramanian P., 2005: “IWAVE: an Ocean simulation model for internal waves”, Current science Vol. 89 No11, 10 December pp 1927-1932

[12] Ramana Murty T.V., Prasanna Kumar S., Somajajulu Y. K., Sastry J S and Rui J P De Figueiredo, 1989:,” Canonical sound speed profile for the central Bay of Bengal”, Earth Planet Sci., Vol.98, No:3, pp.255-263.

[13] Munk W.H and Zachariasen F, 1976:, “Sound propagation through a fluctuating Ocean”: Theory and observations, J. Acoust. Soc. Am. 59, 818-838 .

[14] Flatte M, Dashen R,Munk W.H, Watson W and F.Zachariasen,1979:,” Sound Transmission through a Fluctuating Ocean”, PP.56-57 Cambridge Univ.Press.

[15] Munk, W,H and Wunsch,C., 1979:,” Ocean Acoustic Tomography: A scheme for large scale ocean monitoring”, Deep - Sea Research, 26,123-161.

[16] Moler C.B and Solomon L.P. 1970:, “Use of splines and numerical integration in geometrical acoustics”, JASA 48, p 739.

[17] Urick R.J, “Principles of under water sound”, McGraw-Hill, Inc.,pp.384,1975

[18] Porter M.B., Reiss. E.L., 1984: " A numerical method for ocean acoustic normal modes" J.Acoust.Soc.Am.76,pp244-252.

[19] Porter M.B., 1992:" The Kraken normal mode program ", NRL/MR/5120-92-6920, Naval Research Laboratory, Washington D.C.,

[20] Zhang. R., HeYi and Hong LIU., 1993: " The WKBZ mode approach to sound propagation in range-independent ocean channels", Chinese journal of acoustics Vol. 13 No. 1 pp 1-12.

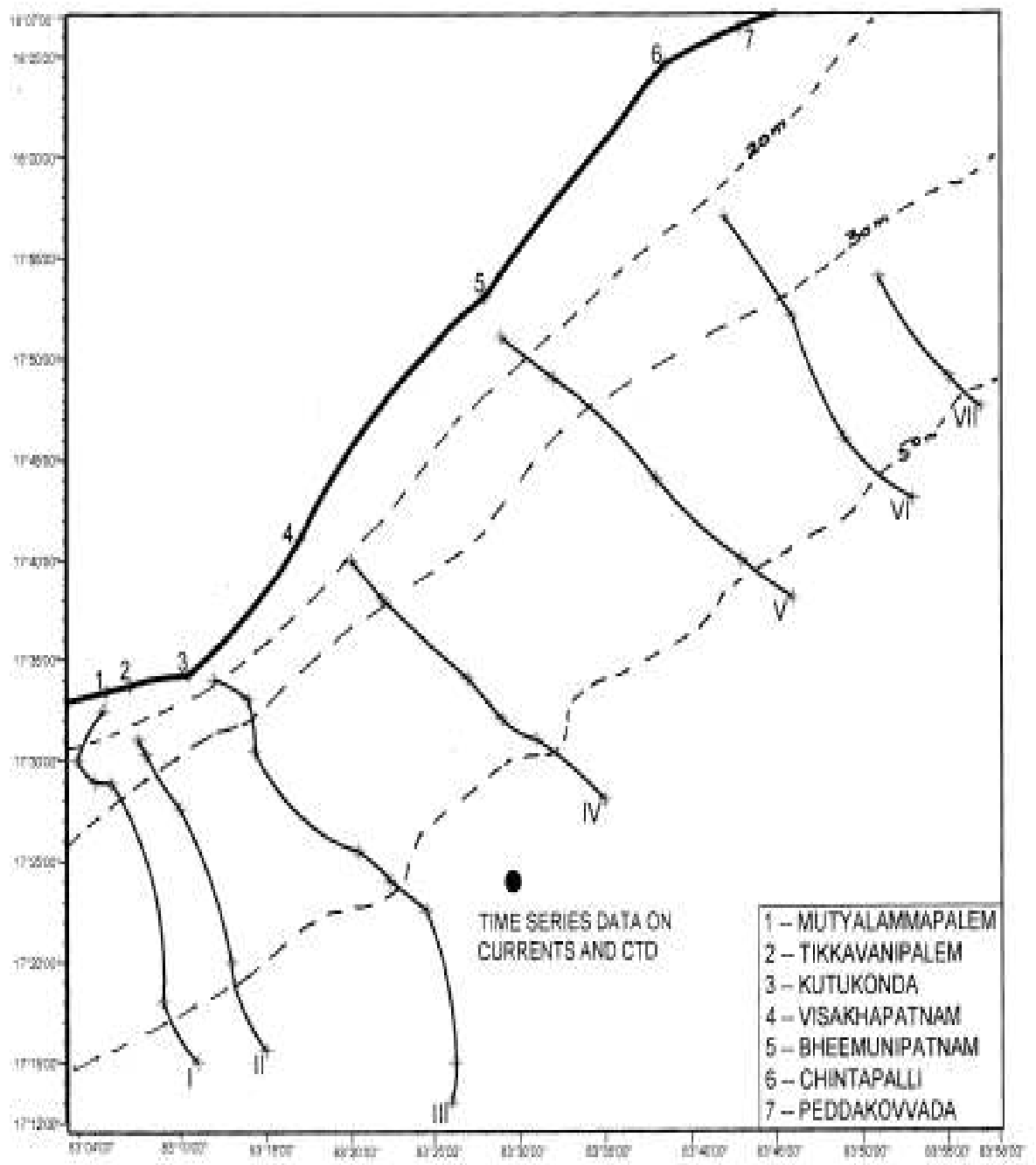
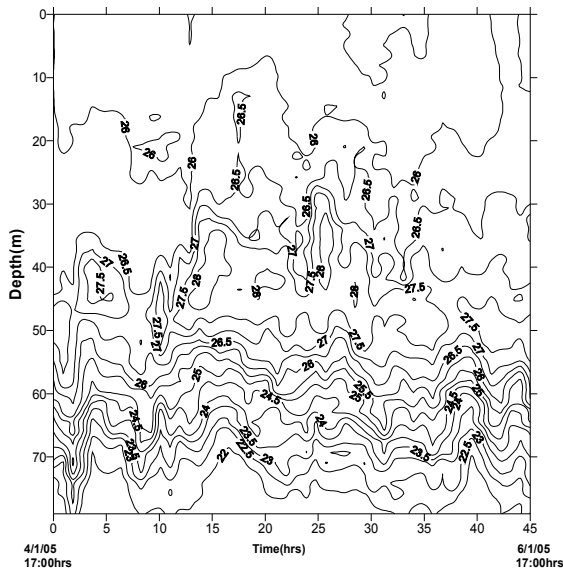
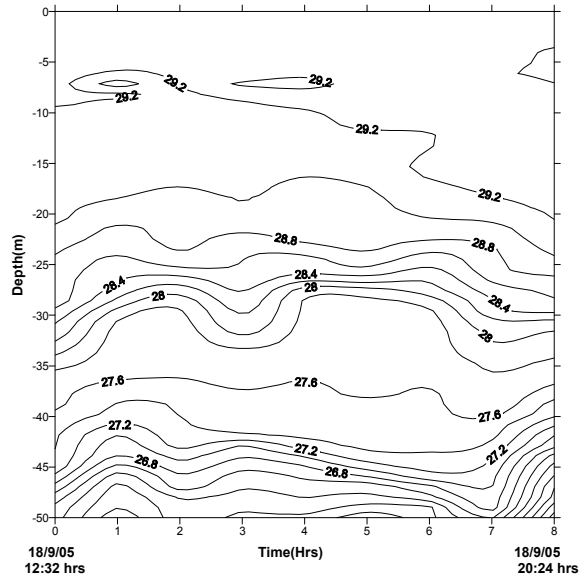


Figure 1: Cruise track of sasu-84 and the fixed location for time series data on currents and CTD

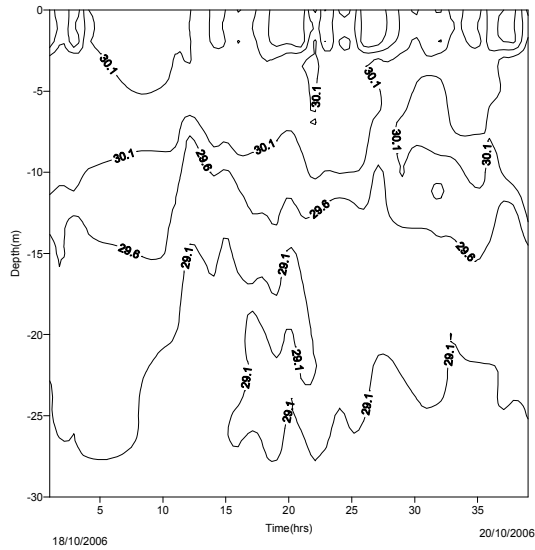
(a) Jan 2005 (VSP)



(b) Sept 2005 (VSP)



(c) Oct 2006 (VSP)



(d) Feb 2007 (Bhimili)

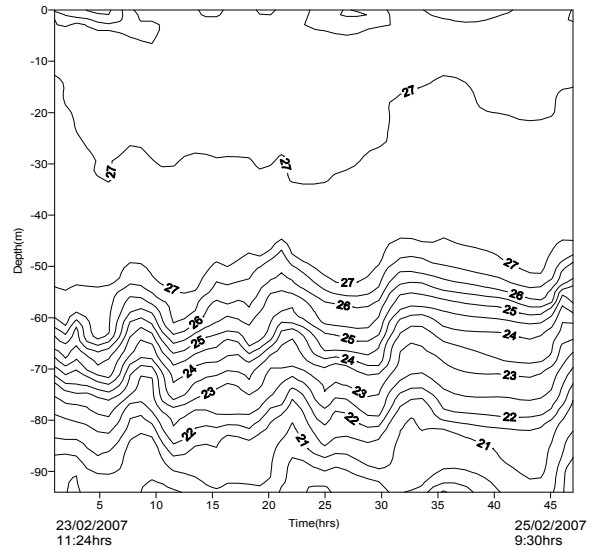
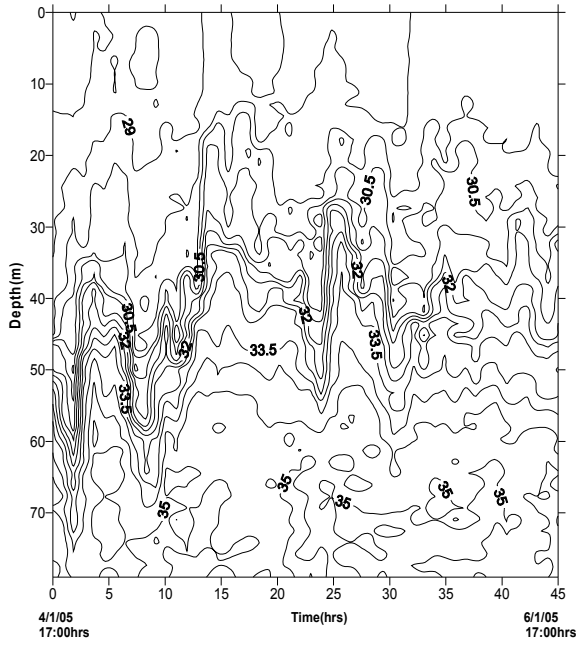
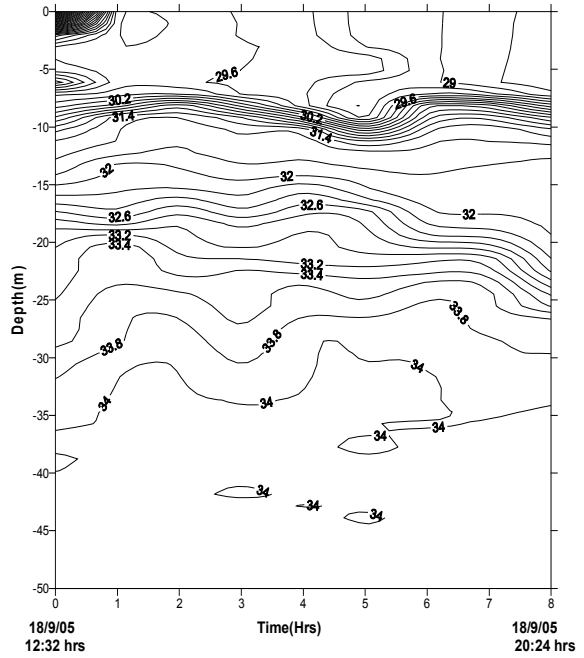


Figure 2: Time series data on temperature ($^{\circ}$ C) off Visakhapatnam (VSP) ($17^{\circ}23.7'N$, $83^{\circ}28.5'E$) and Bhimili ($17^{\circ}35.486'N$, $83^{\circ}42.322'E$)

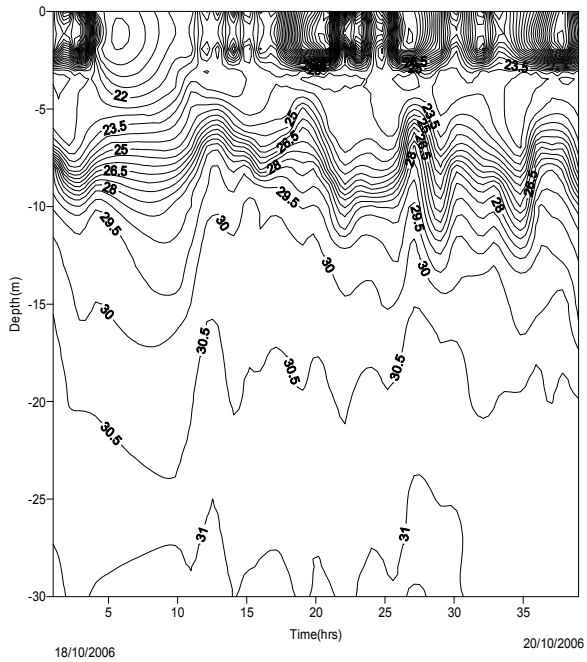
(a) Jan 2005 (VSP)



(b) Sept 2005 (VSP)



(c) Oct 2006 (VSP)



(d) Feb 2007 (Bhimili)

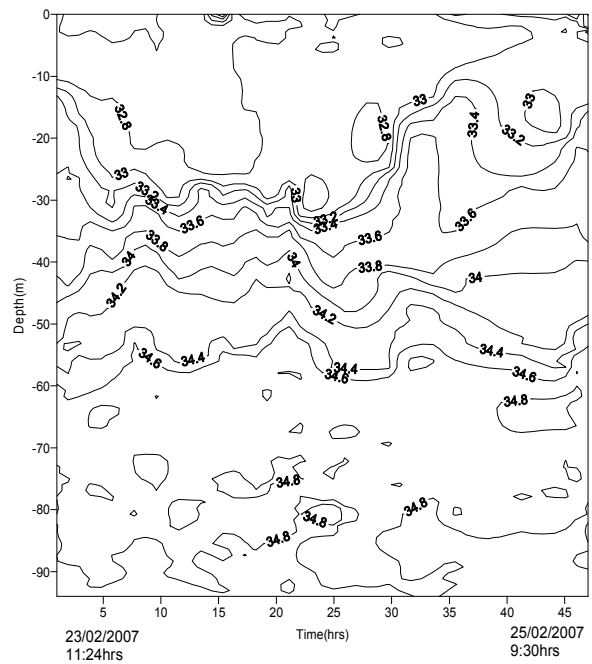
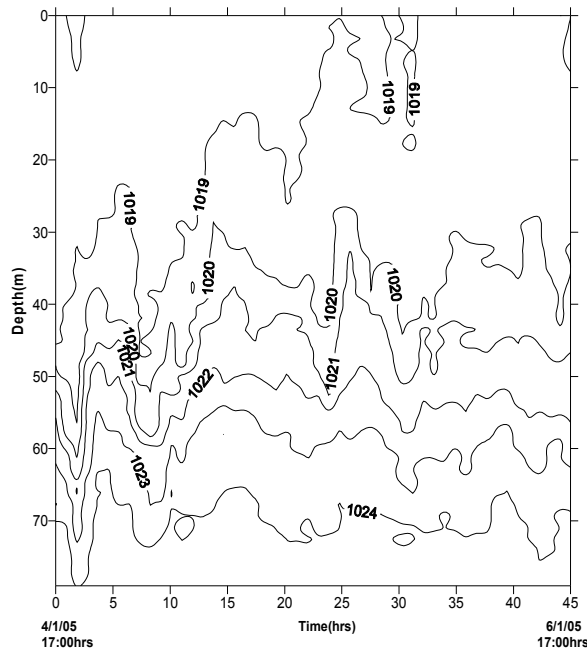
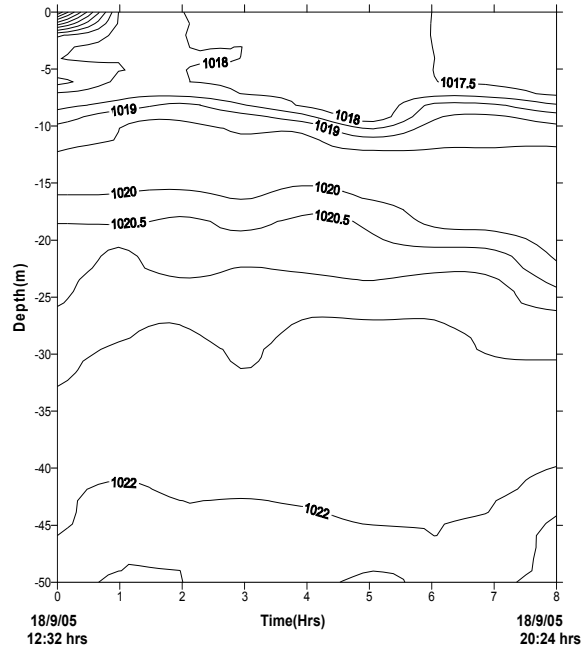


Figure 3: Time series data on salinity (psu) off Visakhapatnam (VSP) ($17^{\circ}23.7'N$, $83^{\circ}28.5'E$) and Bhimili ($17^{\circ}35.486'N$, $83^{\circ}42.322'E$)

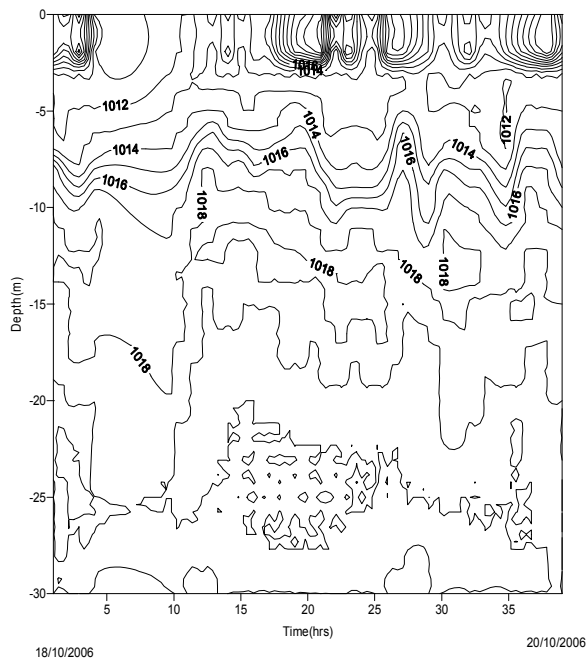
(a) Jan 2005 (VSP)



(b) Sept 2005 (VSP)



(c) Oct 2006 (VSP)



(d) Feb 2007 (Bhimili)

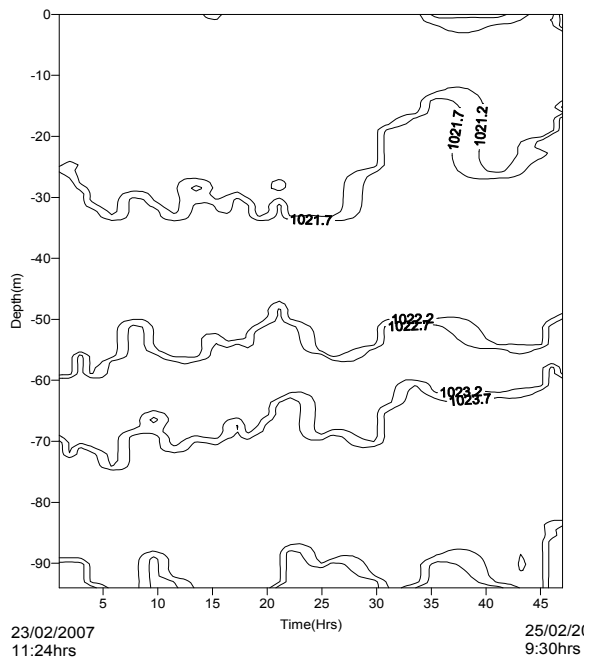
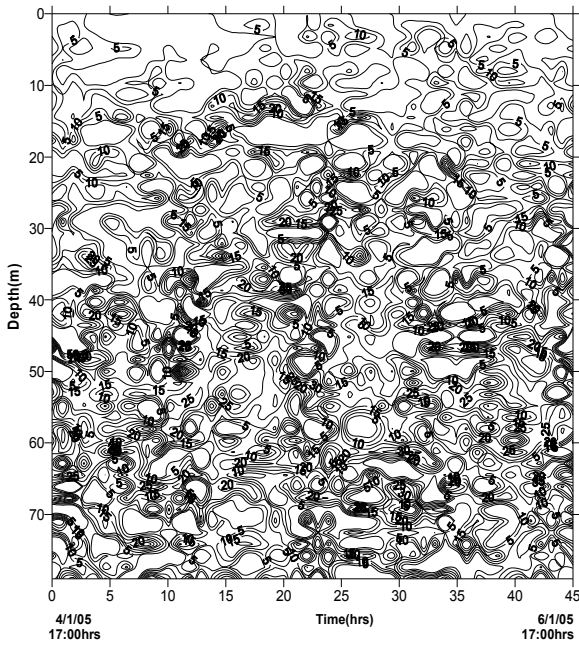
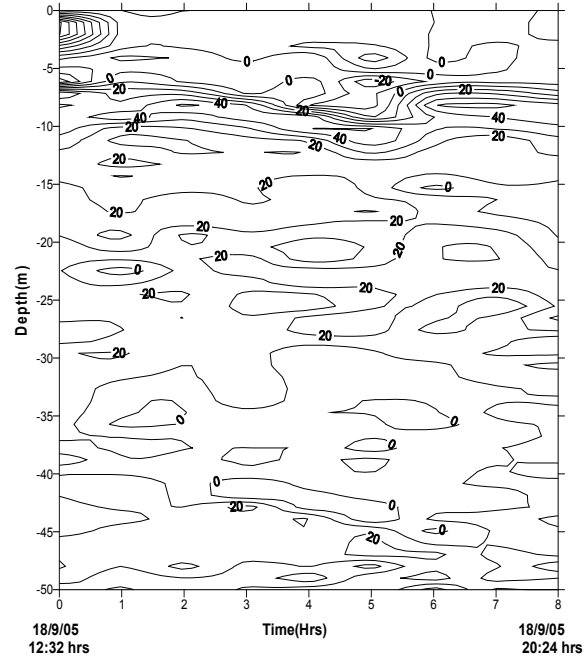


Figure 4: Time series data on density (kg/m^3) off Visakhapatnam (VSP) ($17^{\circ}23.7'N$, $83^{\circ}28.5'E$) and Bhimili ($17^{\circ}35.486'N$, $83^{\circ}42.322'E$)

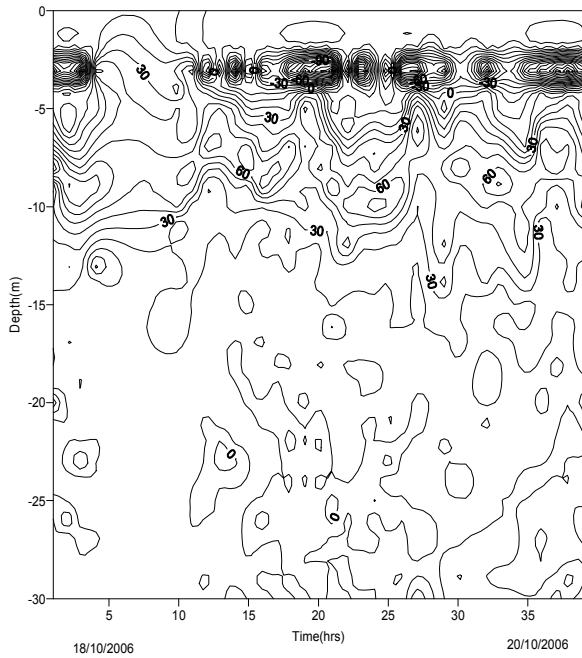
(a) Jan 2005 (VSP)



(b) Sept 2005 (VSP)



(c) Oct 2006 (VSP)



(d) Feb 2007 (Bhimili)

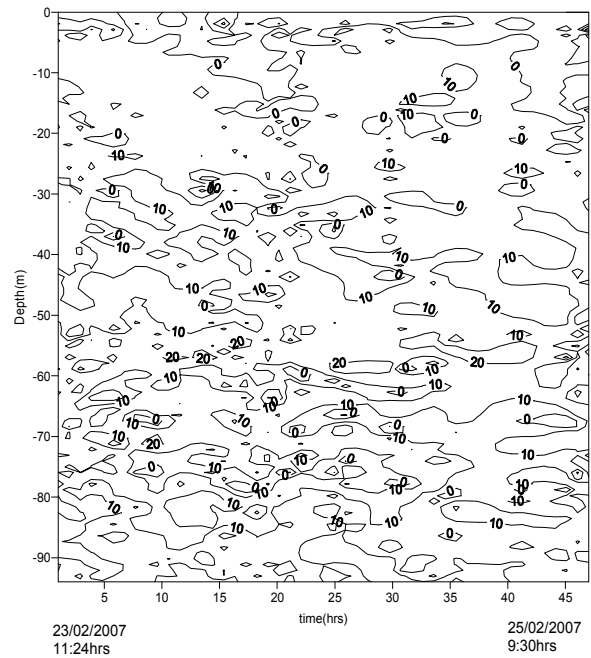


Figure 5: Variation of Brunt-Viasala's frequency (cph) off Visakhapatnam (VSP) ($17^{\circ}23.7'N$, $83^{\circ}28.5'E$) and Bhimili ($17^{\circ}35.486'N$, $83^{\circ}42.322'E$)

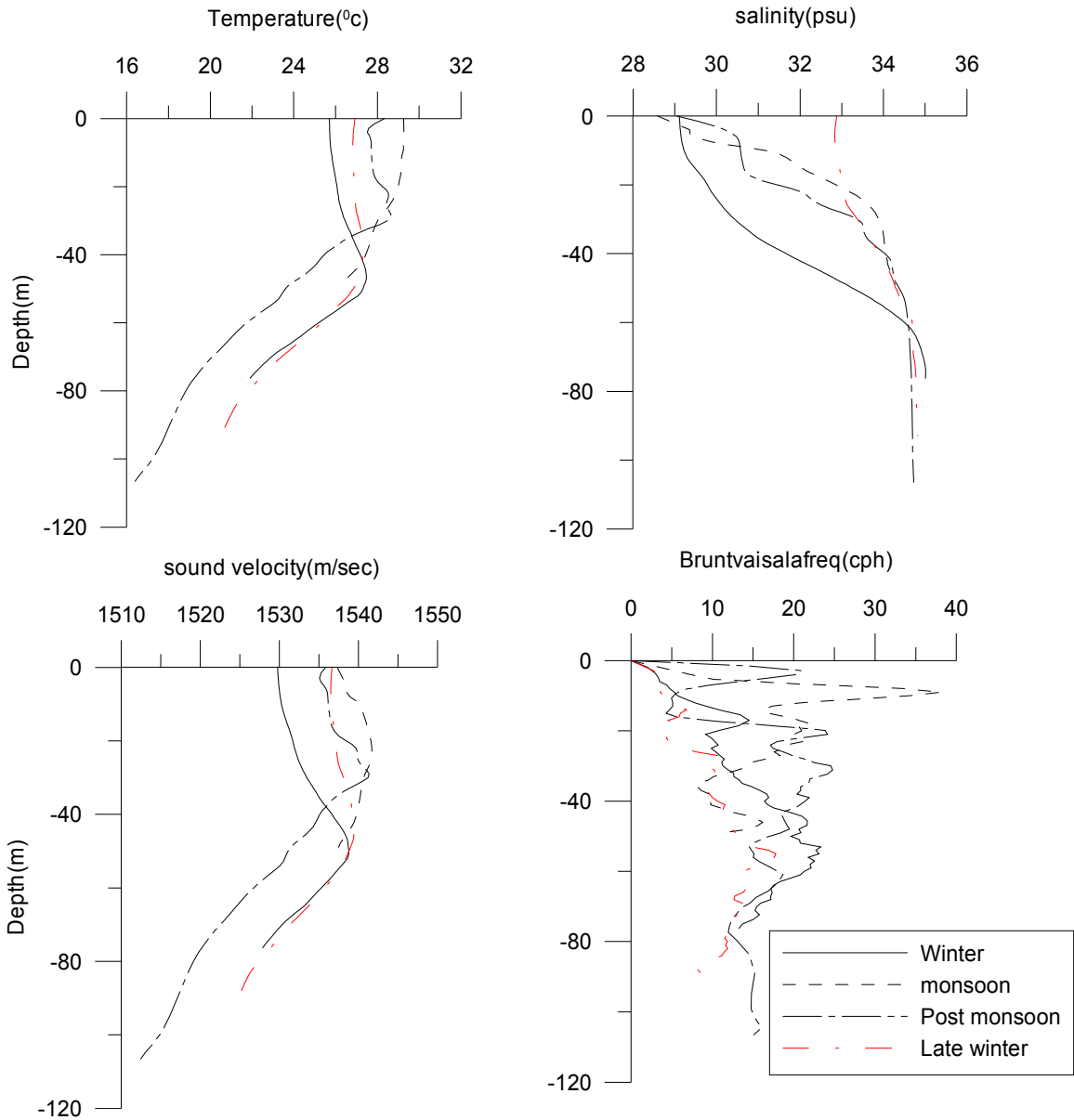
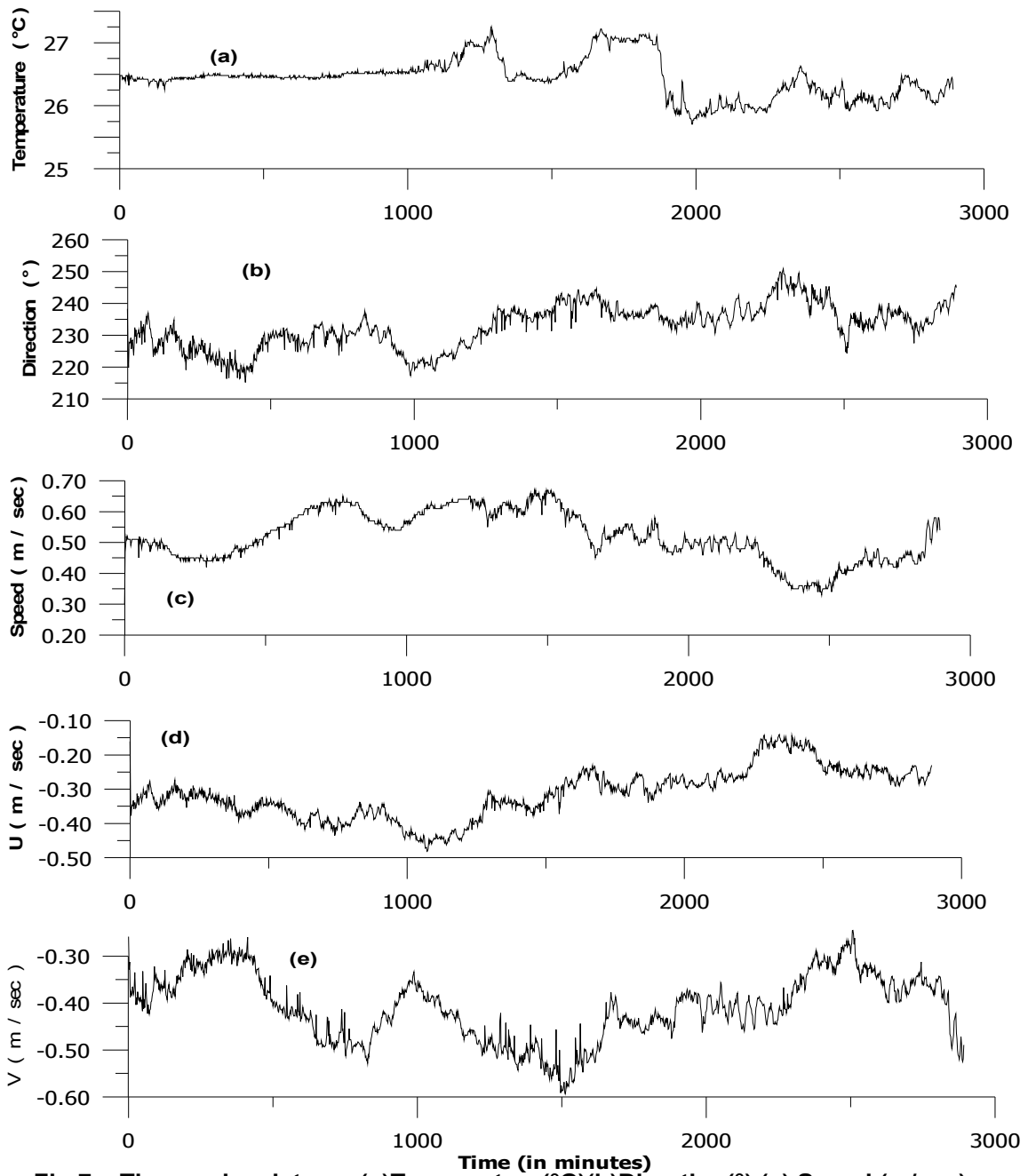


Figure 7: Mean vertical distribution of a) temperature ($^{\circ}\text{C}$) b) salinity (psu) (c) density (kg / m^3) d) sound velocity (m/sec) e) Brunt-viasala's frequency (cph) off Visakhapatnam during 4 January, 18 September 2005 and 18 October 2006

Jan 2005 (VSP)

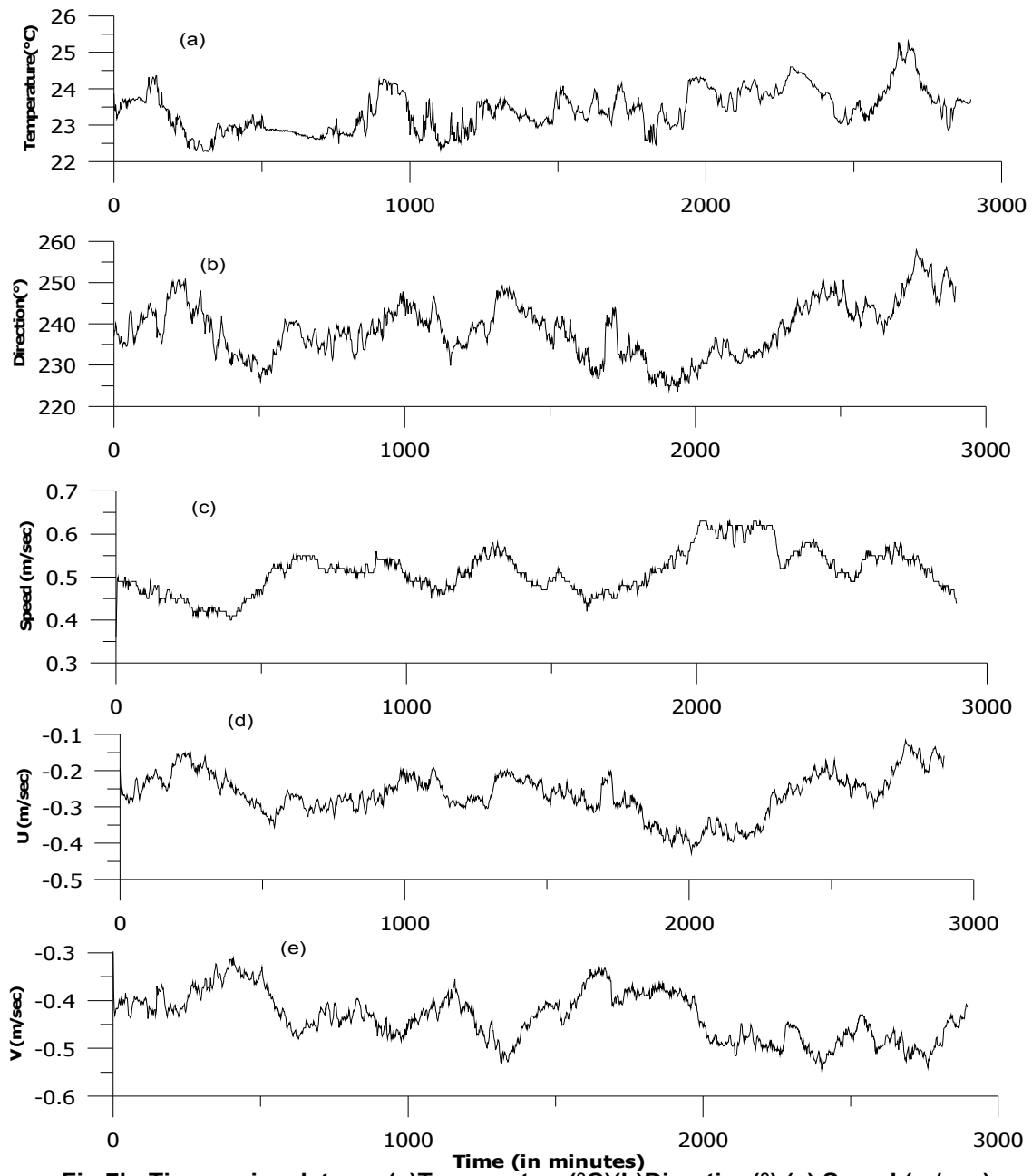


4/1/05
17:00hrs

6/1/05
17:30hrs

Figure 8(a): Time series data on (a) temperature ($^{\circ}\text{C}$) (b) direction ($^{\circ}$) (c) speed (m/sec) (d) U-component (m/sec) (e) V-component (m/sec) at 10m depth off Visakhapatnam (VSP)

Jan 2005 (VSP)



4/1/05
17:00hrs

6/1/05
17:30hrs

Figure 8(b): Time series data on (a) temperature ($^{\circ}\text{C}$) (b) direction ($^{\circ}$) (c) speed (m/sec) (d) U-component (m/sec) (e) V-component (m/sec) at 60m depth off Visakhapatnam (VSP)

Sept 2005 (VSP)

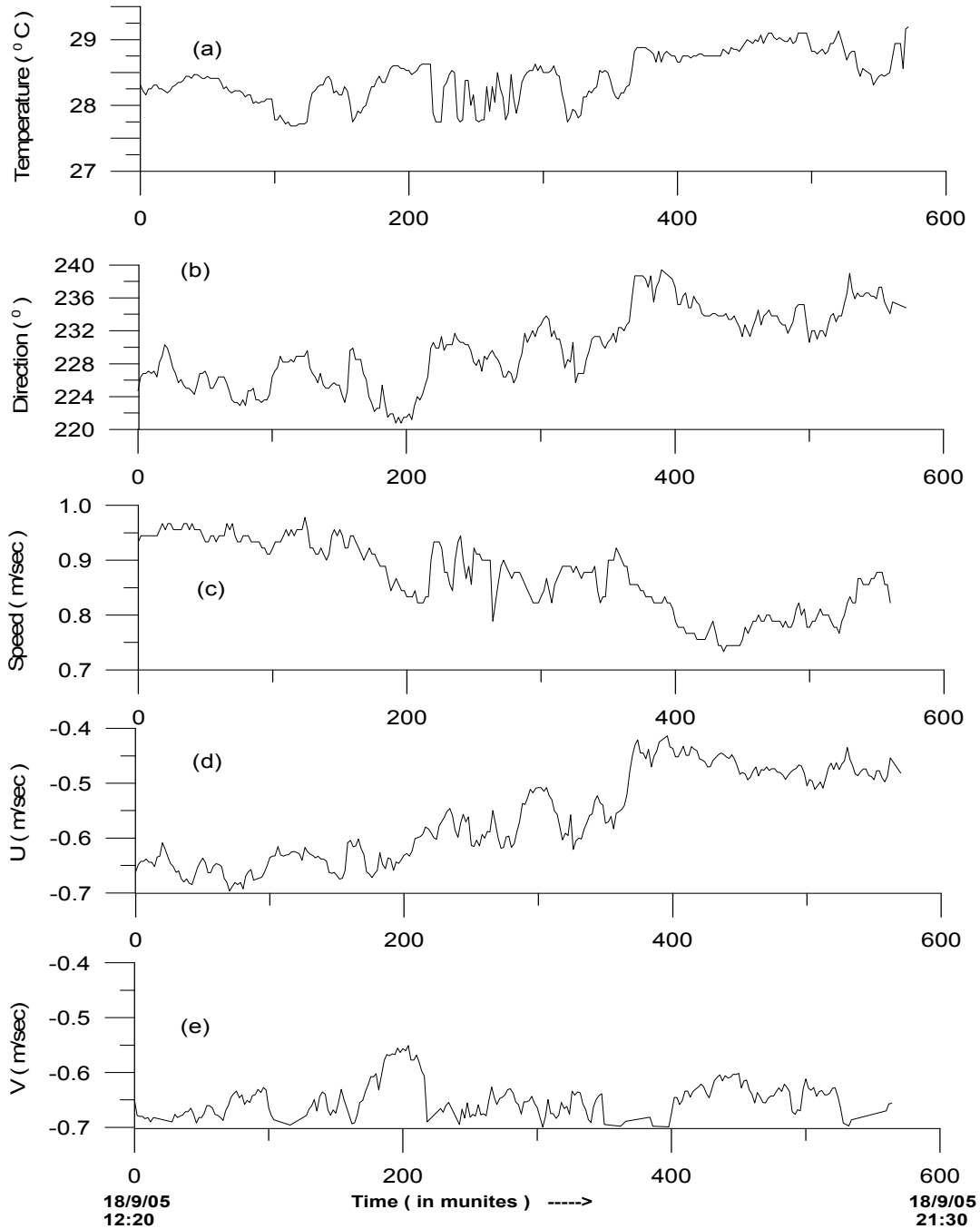


Figure 8(c): Time series data on (a) temperature ($^{\circ}\text{C}$) (b) direction ($^{\circ}$) (c) speed (m/sec) (d) U-component (m/sec) (e) V-component (m/sec) at 10m depth off Visakhapatnam (VSP)

Sept 2005 (VSP)

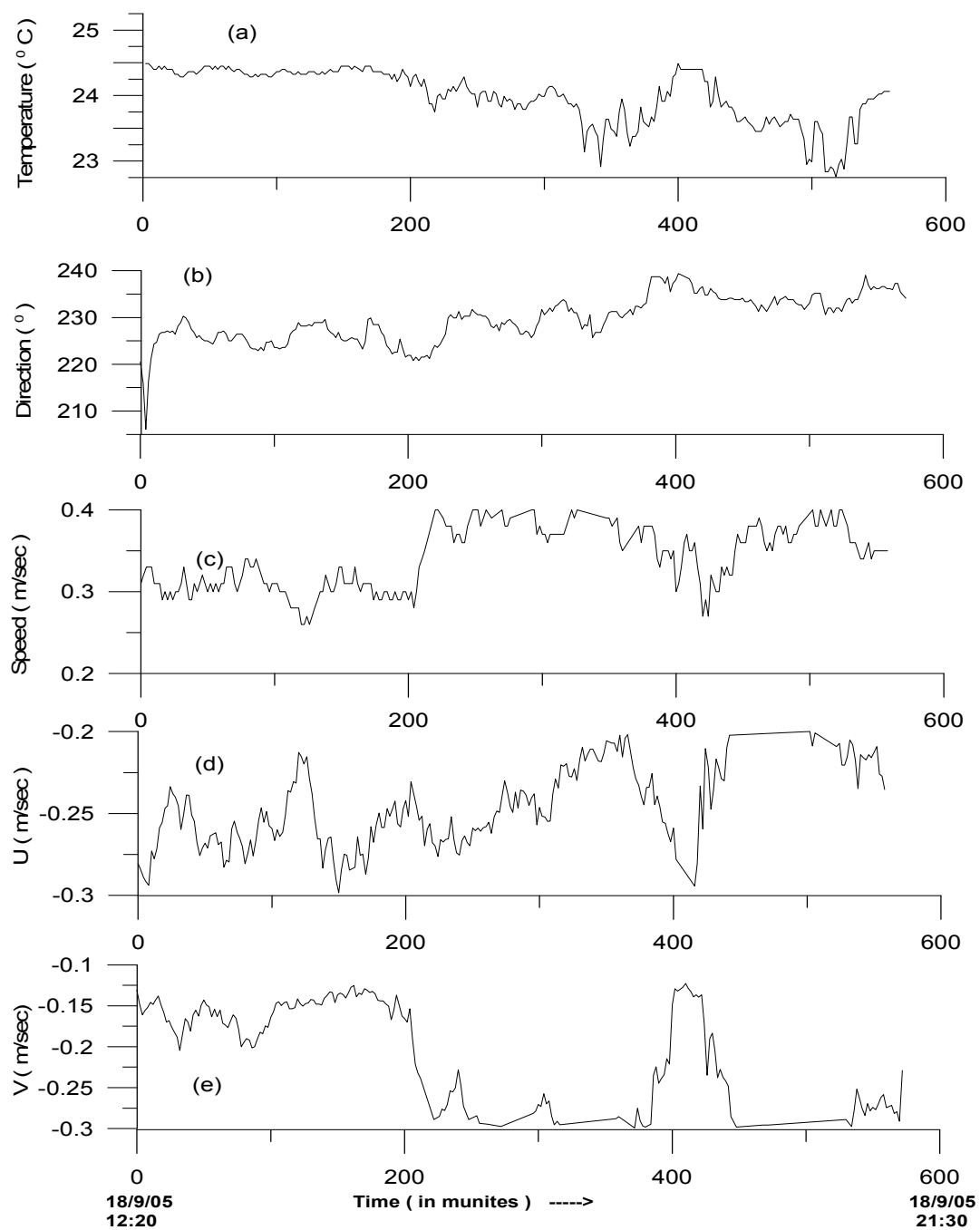


Figure 8(d): Time series data on (a) temperature ($^{\circ}\text{C}$) (b) direction ($^{\circ}$) (c) speed (m/sec) (d) U-component (m/sec) (e) V-component (m/sec) at 60m depth off Visakhapatnam (VSP)

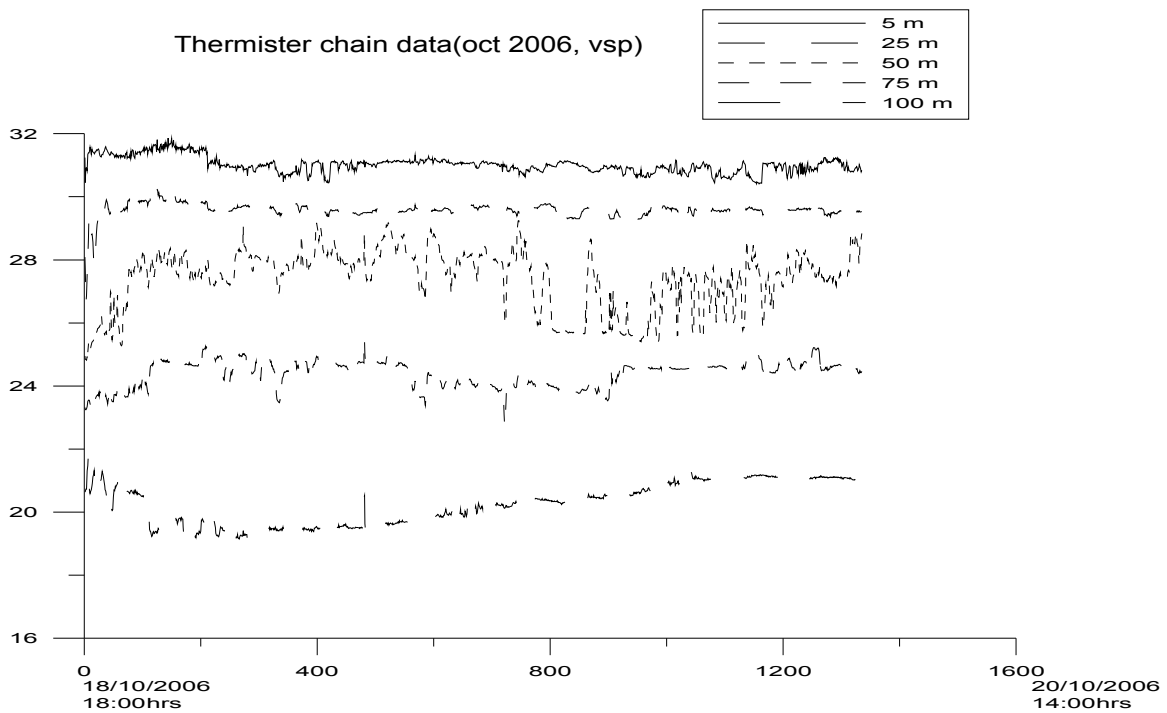


Figure 9(a): Time series data on temperature (2 minute) collected from thermister chain at off Visakhapatnam during 18-20 oct2006

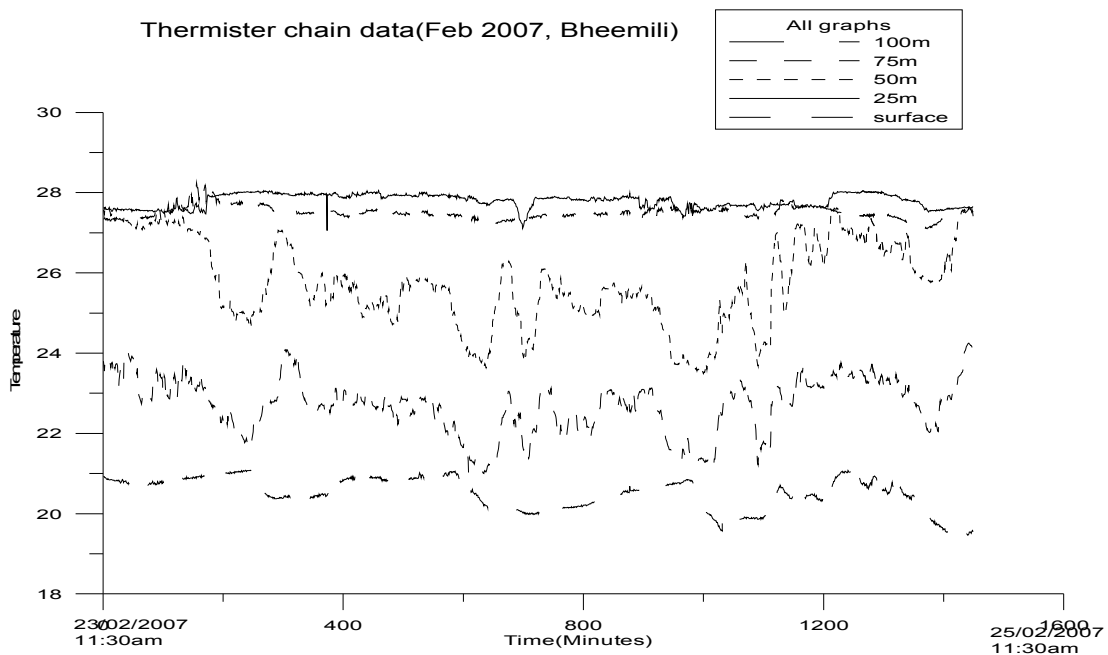


Figure 9(b): Time series data on temperatures (2 minute) collected from thermister chain at off Bhimili during 23-25 Feb2007

Current meter data

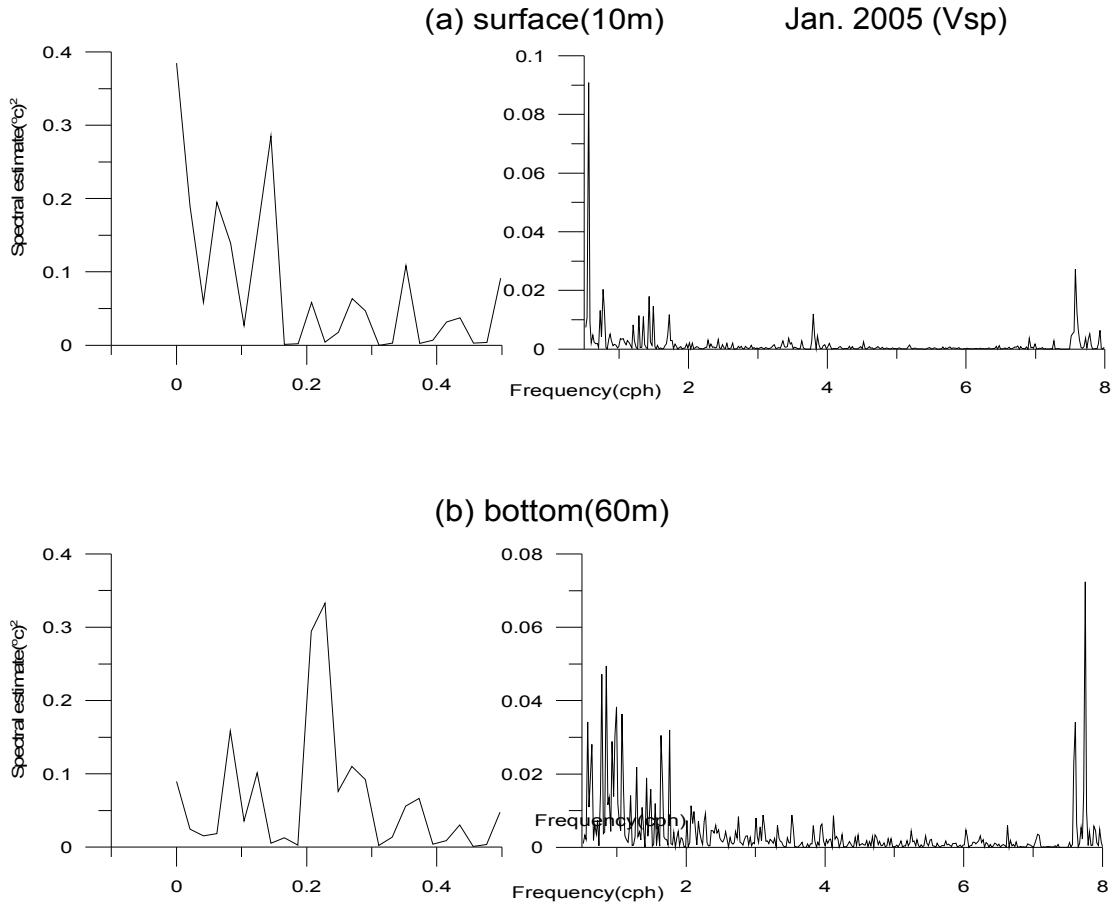
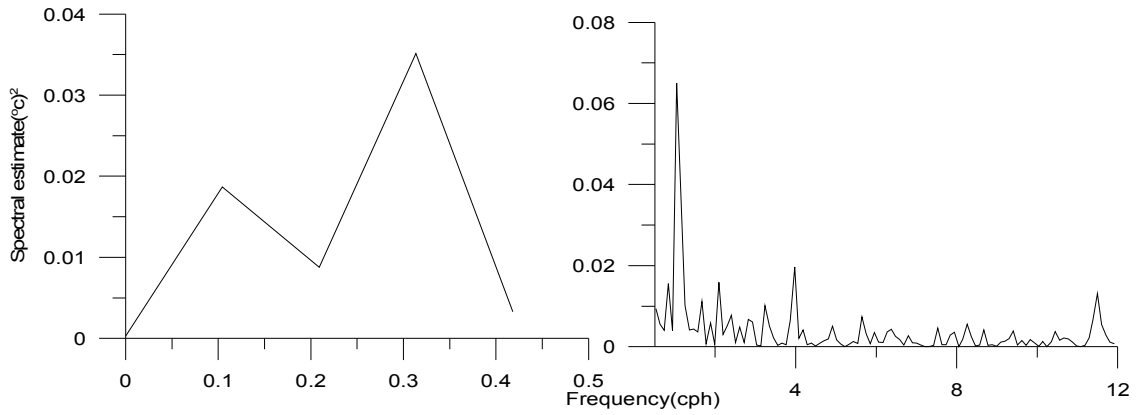


Figure 10(a): Energy density spectra of temperature oscillations at a) 10m and b) 60m off Visakhapatnam (VSP) during 4/1/05 to 6/1/05

(a) surface(10m) Sept 2005 (Vsp)



(b) bottom (60m)

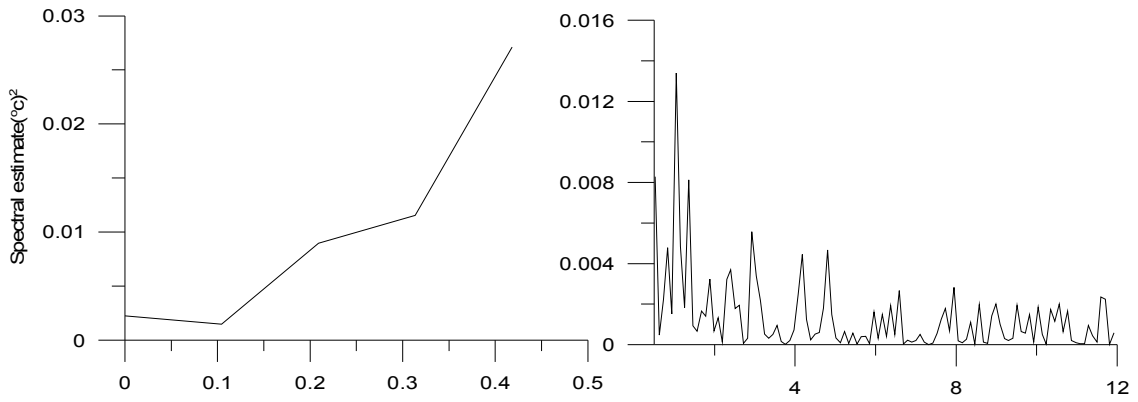


Figure 10(b): Energy density spectra of temperature oscillations at a) 10m and b) 60m off Visakhapatnam VSP) during 18/9/05

Thermister chain and current meter data (10m & 60m) Oct 2006 (VSP)

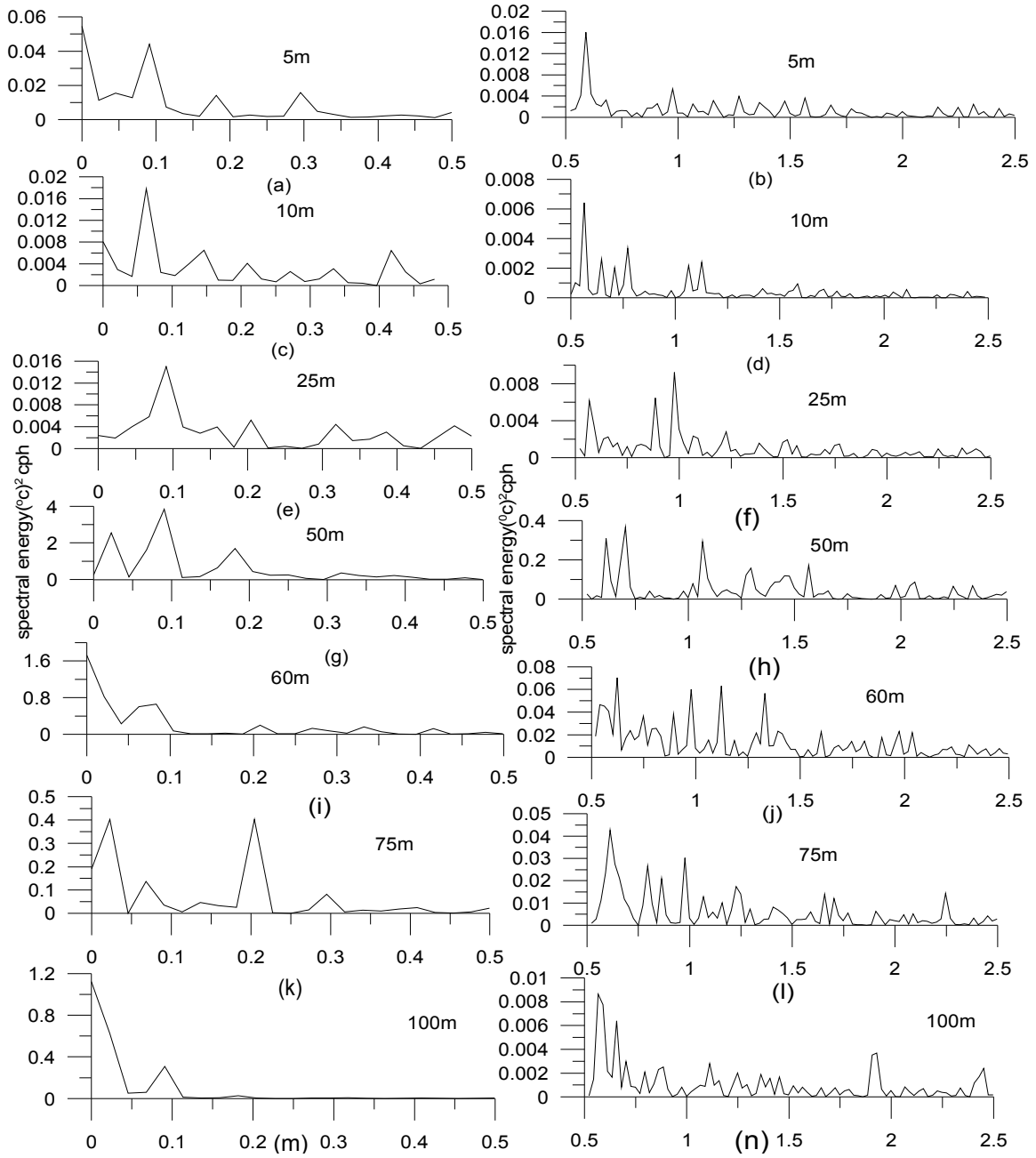


Figure 10(c): Energy spectra of temperature oscillations at depths 5m, 10m, 25m, 50m, 75m, 100m off Visakhapatnam (VSP) during 18-20 Oct 2006

Thermister chain data (Feb 2007, Bhimili)

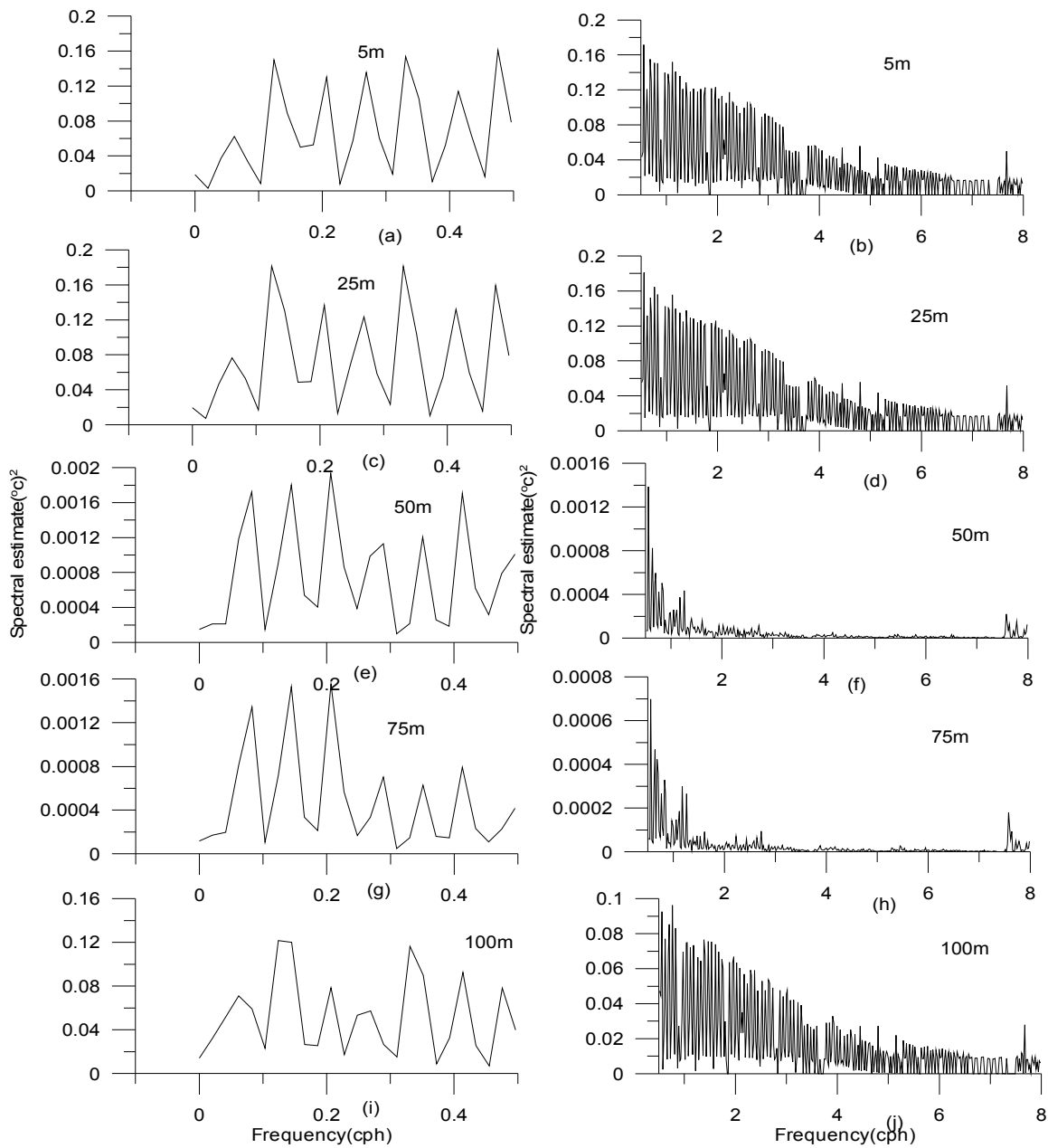


Figure 10(d): Energy spectra of temperature oscillations at depths 5m, 25m, 50m, 75m and 100m off Bhimili during 23-25 Feb2007

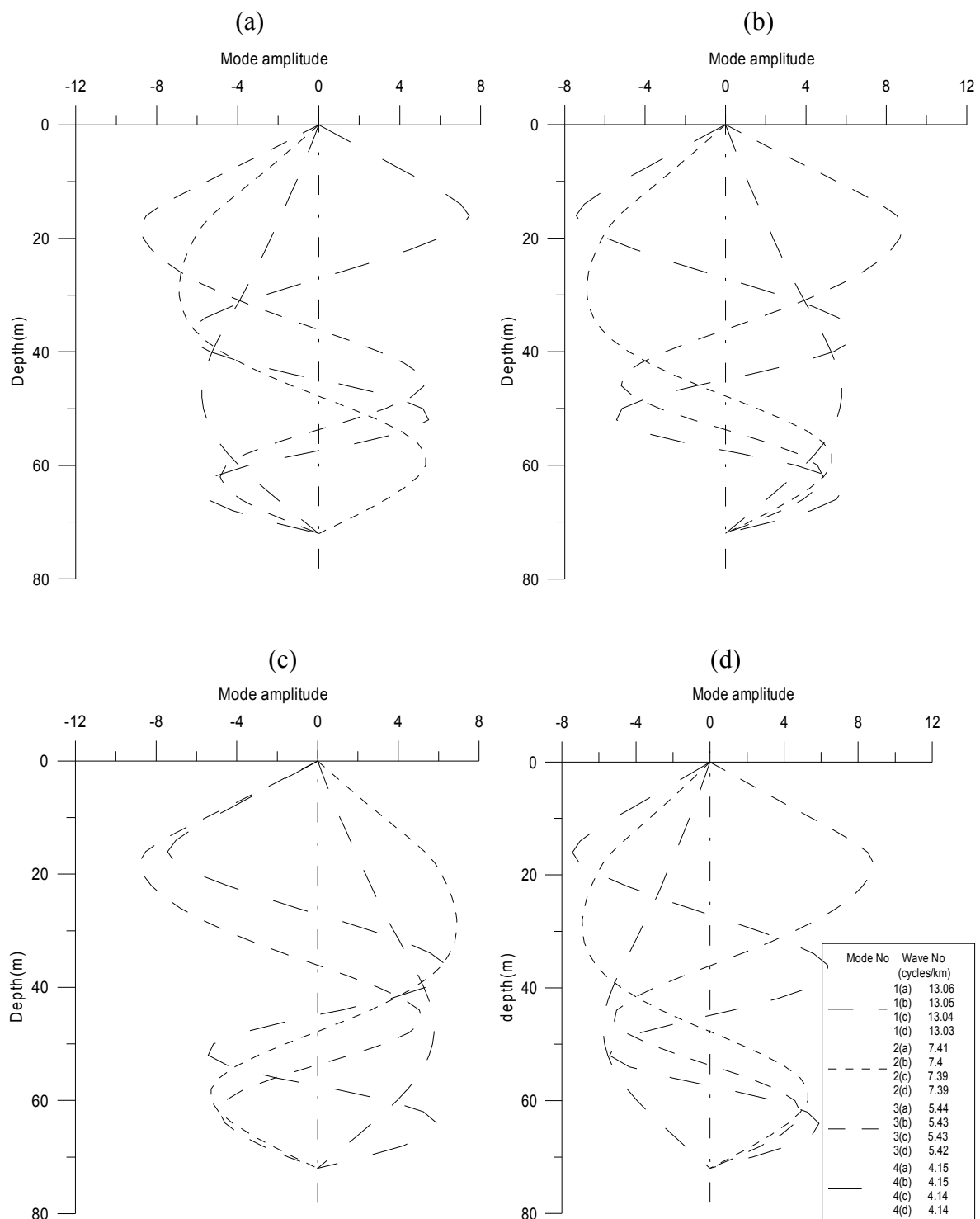


Figure 11(a): Internal wave modes for frequencies (cph) (a) 8 (b) 7.99 (c) 7.98 (d) 7.97 off Visakhapatnam during January 2005

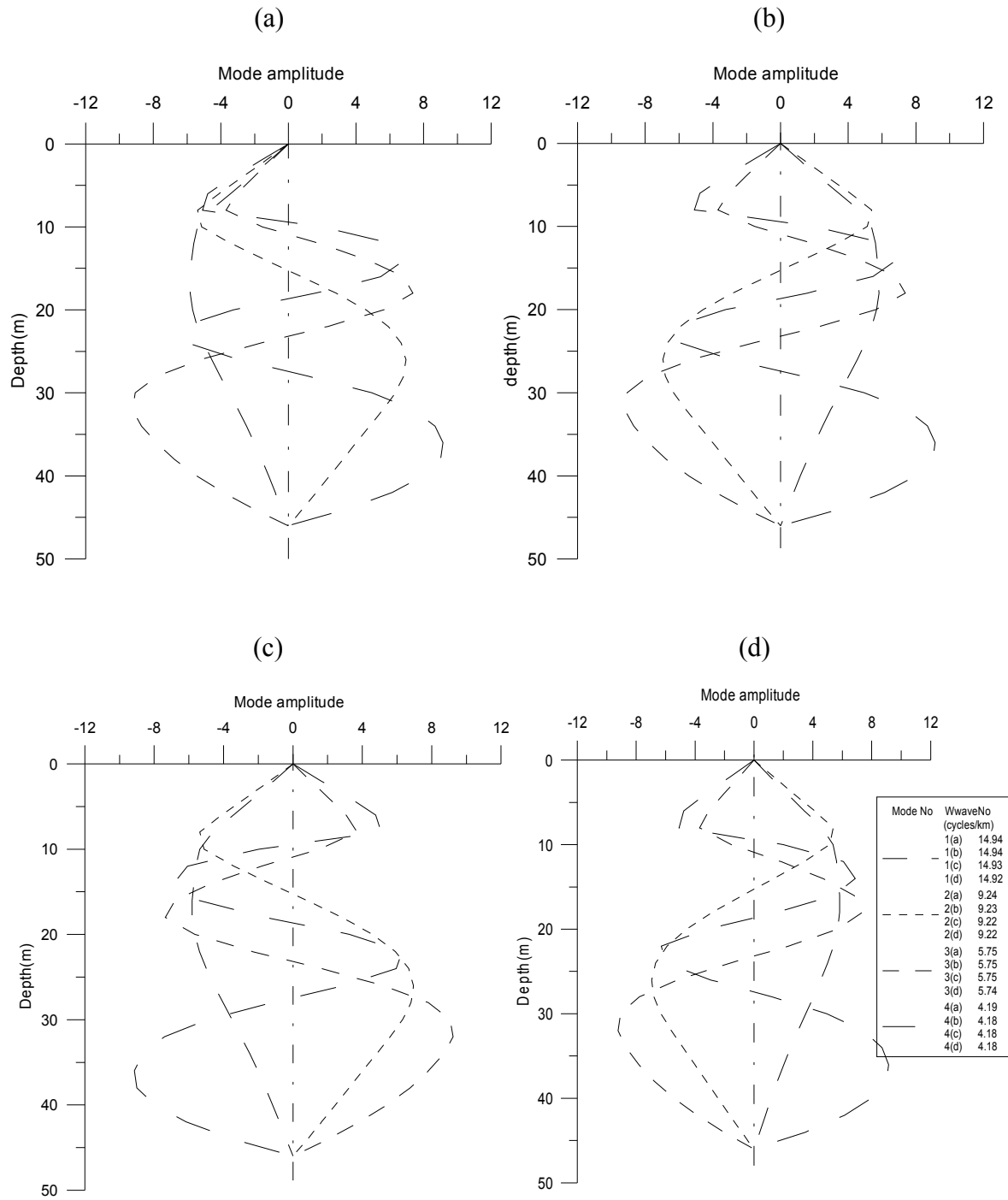


Figure 11(b): Internal wave modes for frequencies (cph) (a) 1.5 (b) 1.49 (c) 1.48 (d) 1.47 off Visakhapatnam during September 2005

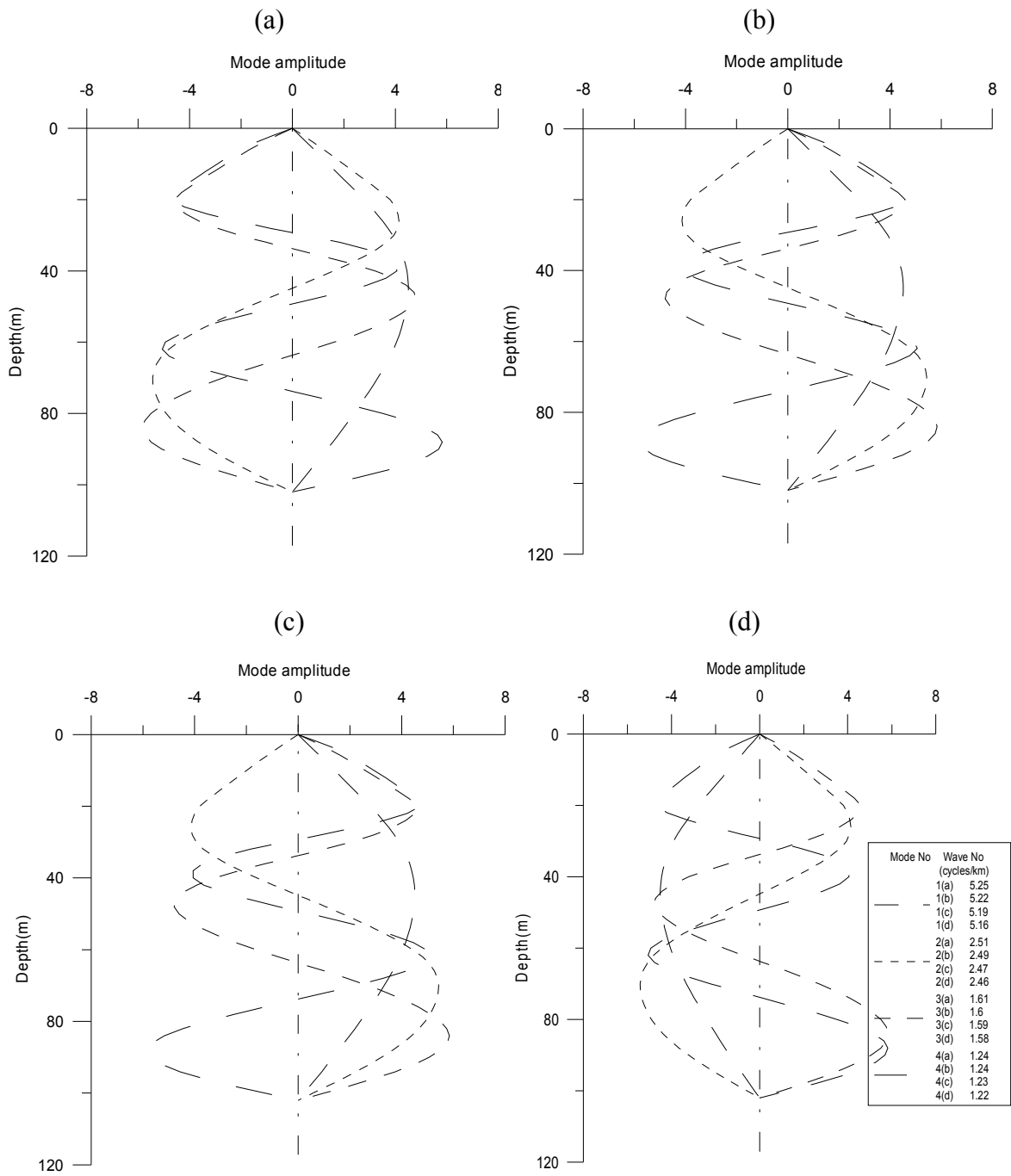


Figure 11(c): Internal wave modes for frequencies (cph) (a) 1.5 (b) 1.49 (c) 1.48 (d) 1.47 off Visakhapatnam during October 2006

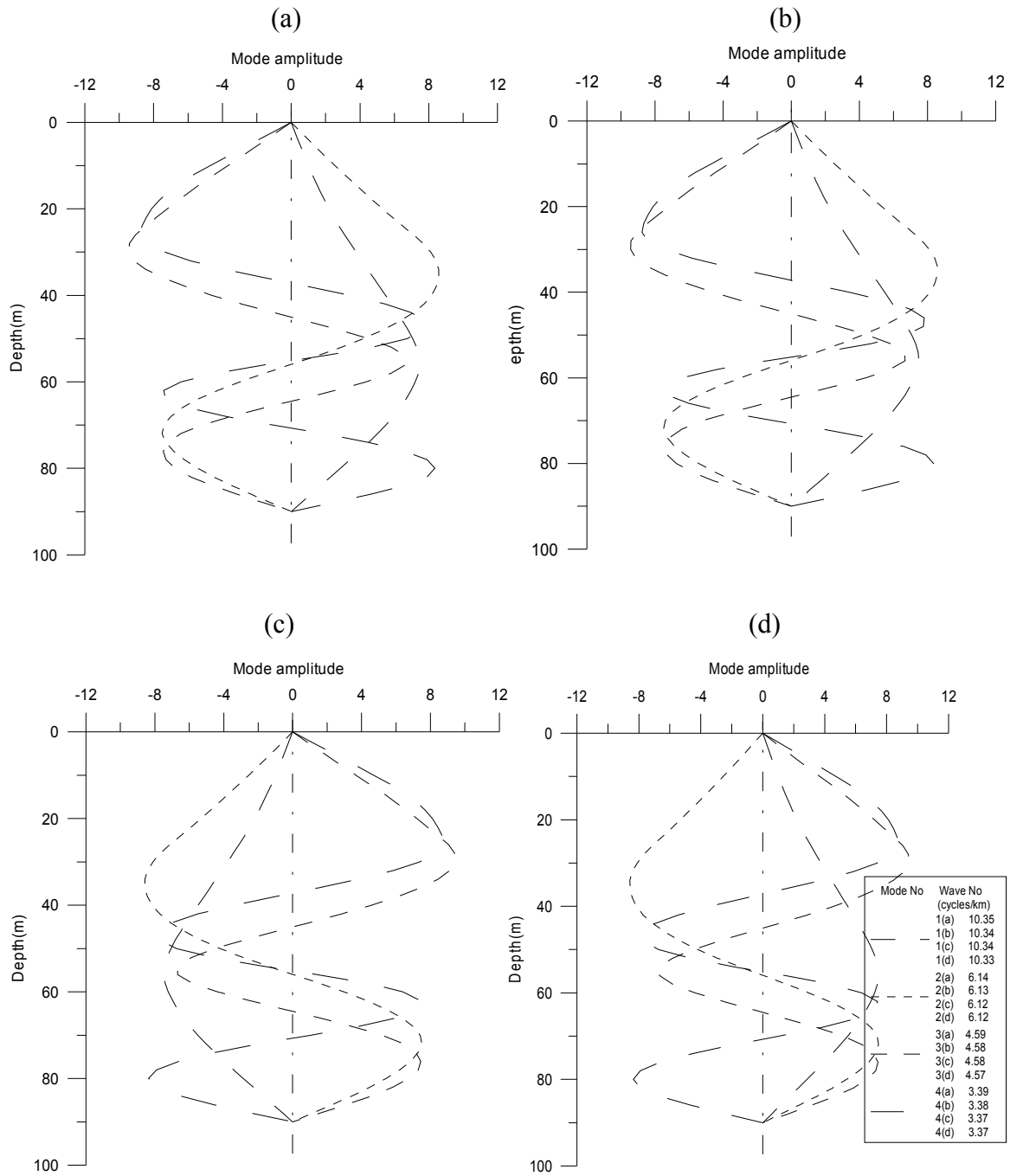


Figure 11(d): Internal wave modes for frequencies (cph) (a) 8 (b) 7.99 (c) 7.98 (d) 7.97 off Visakhapatnam during February 2007

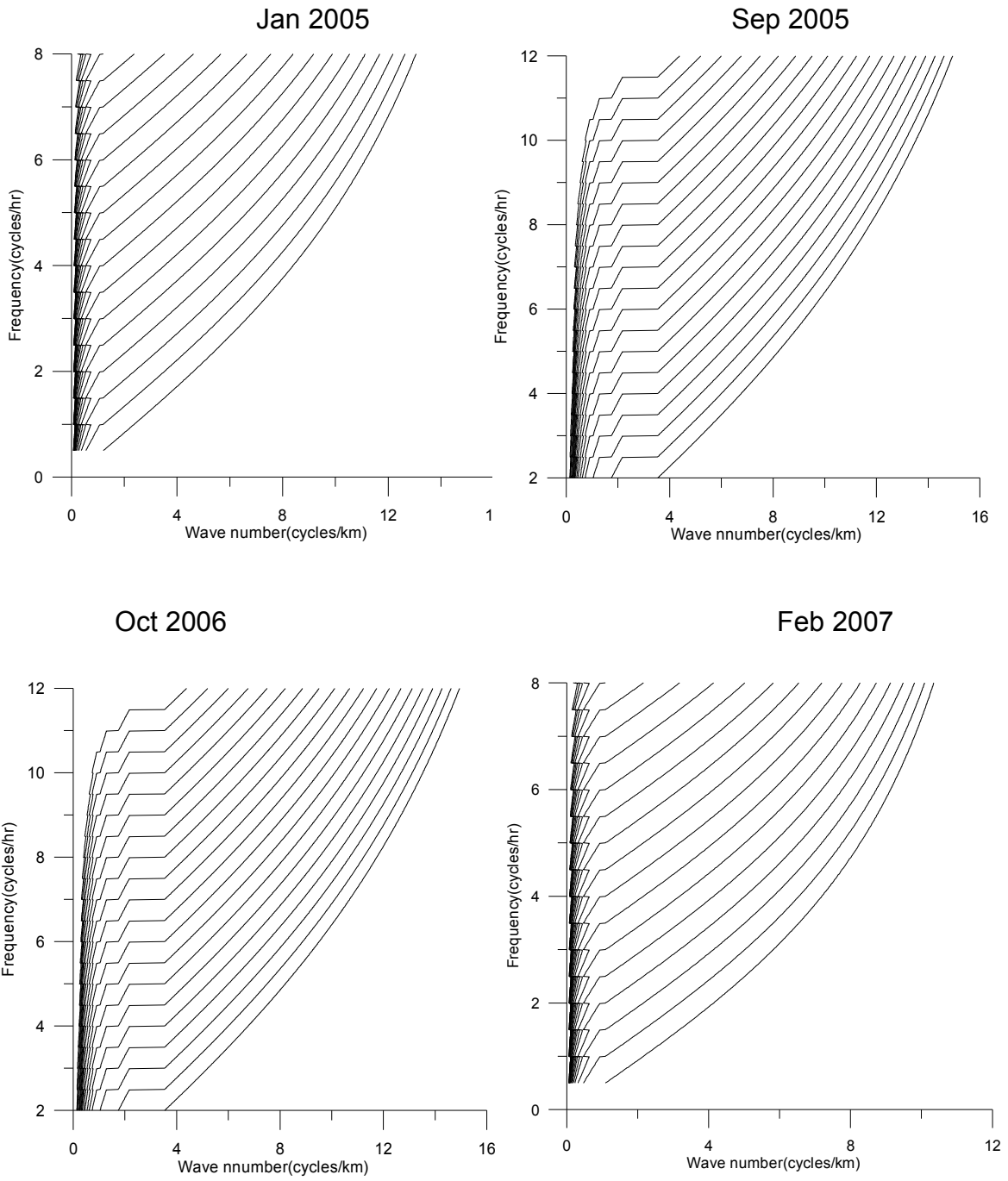
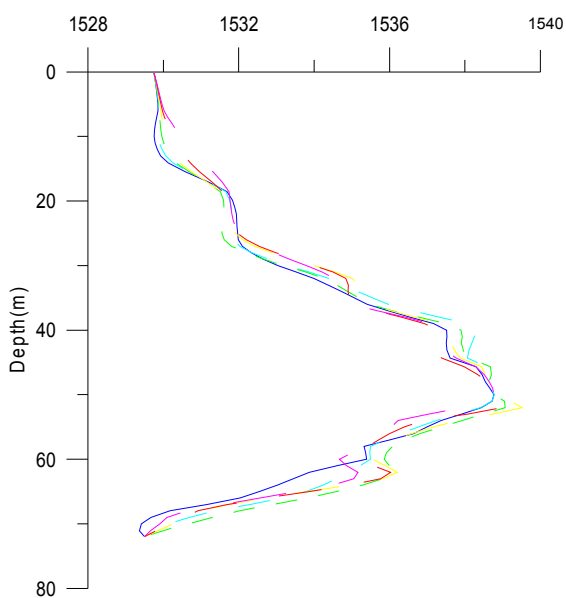
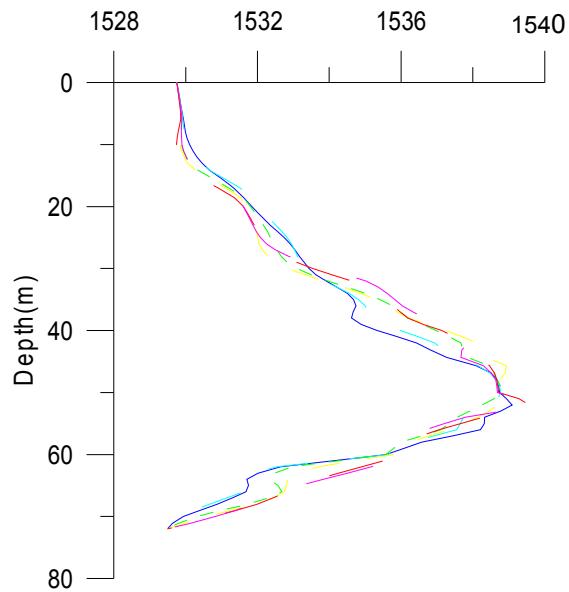


Figure 12: Internal wave dispersion relations

Jan 2005

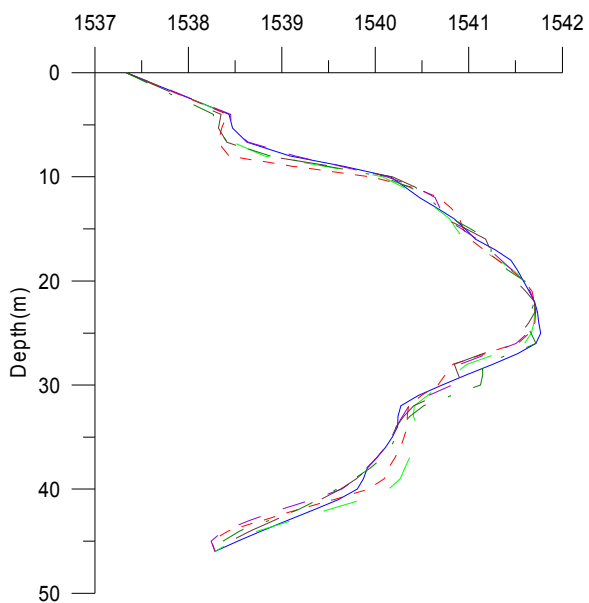


Sound speed (m/sec)

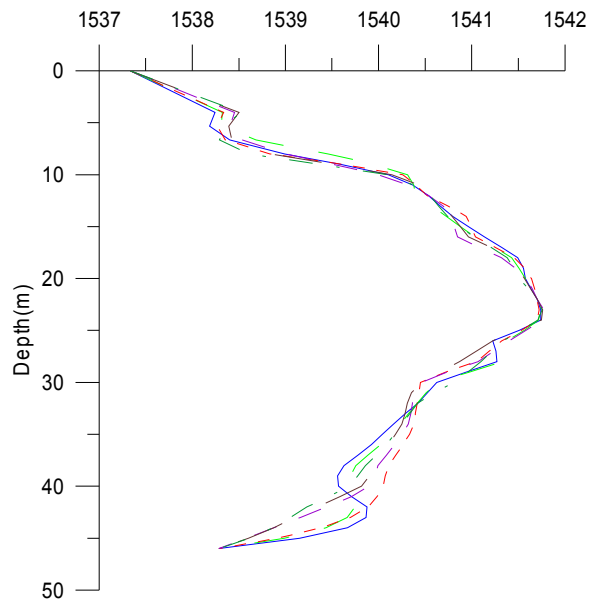


Sound speed (m/sec)

Sep 2005

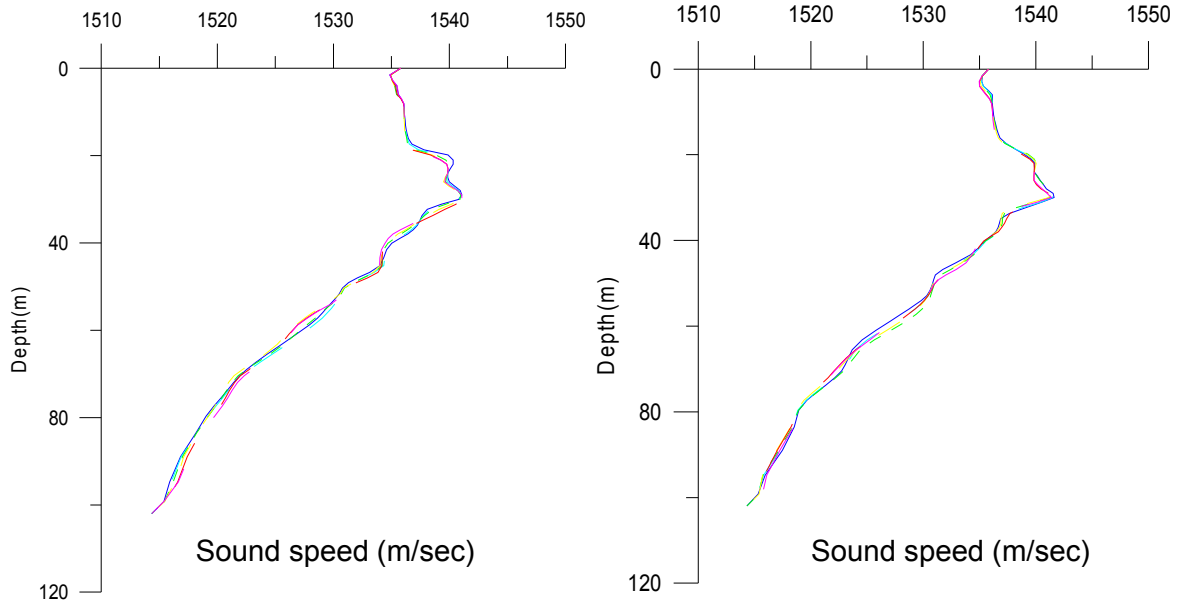


Sound speed (m/sec)



Sound speed (m/sec)

Oct 2006



Feb 2007

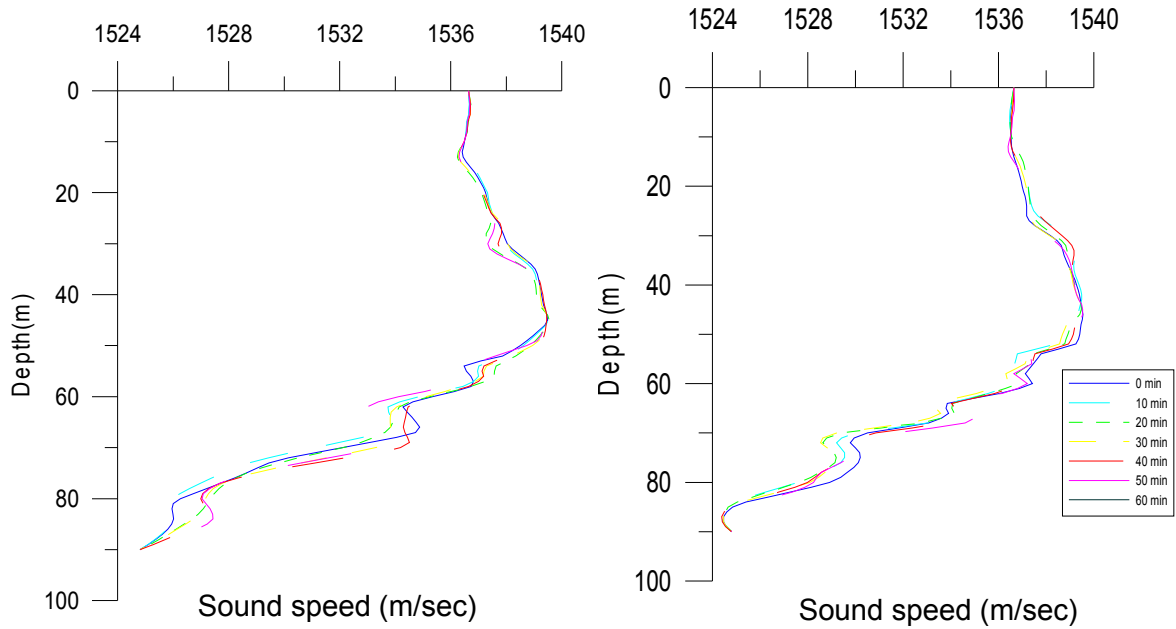
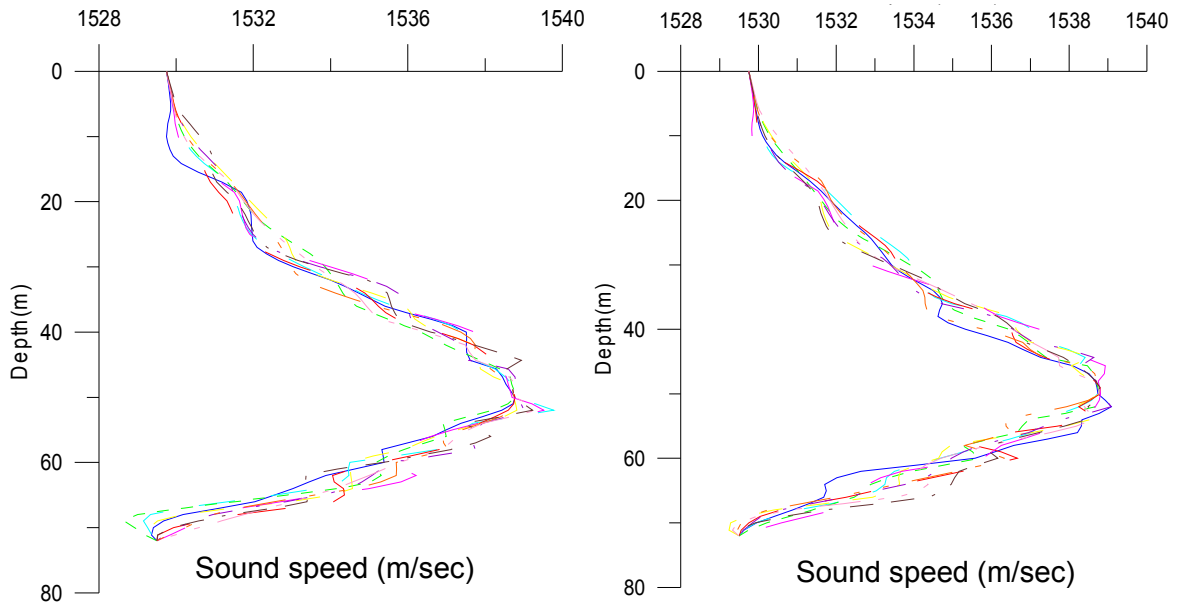
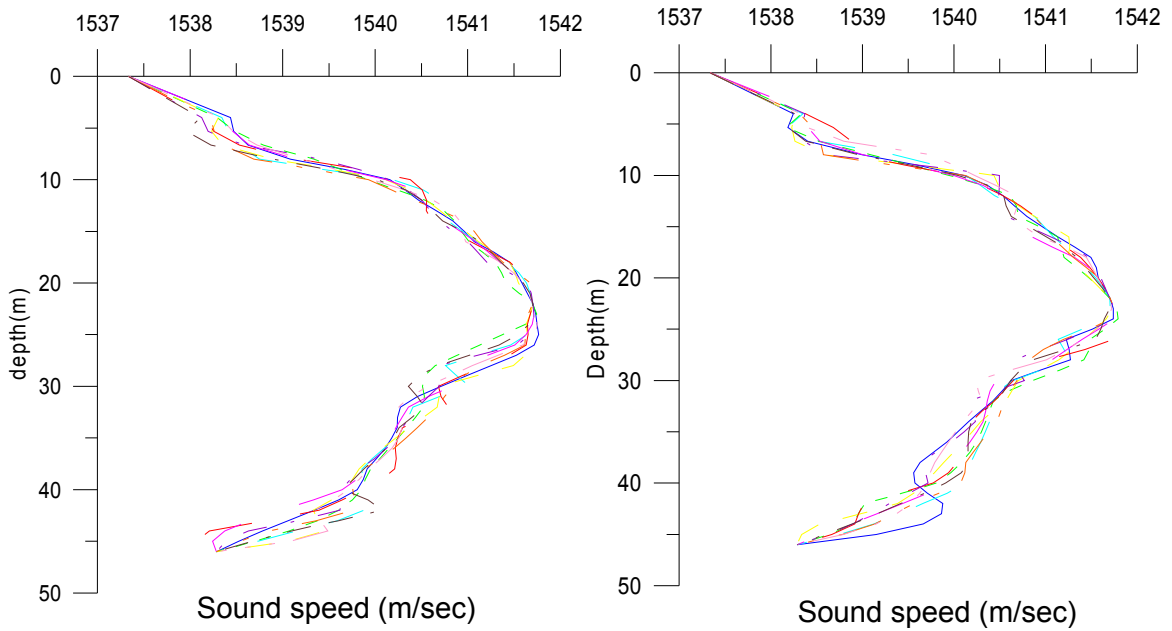


Figure13: Sound velocity relations (a- single b-double) in 50 min, 10 min apart off VSP and Bhimili

Jan 2005



Sep 2005



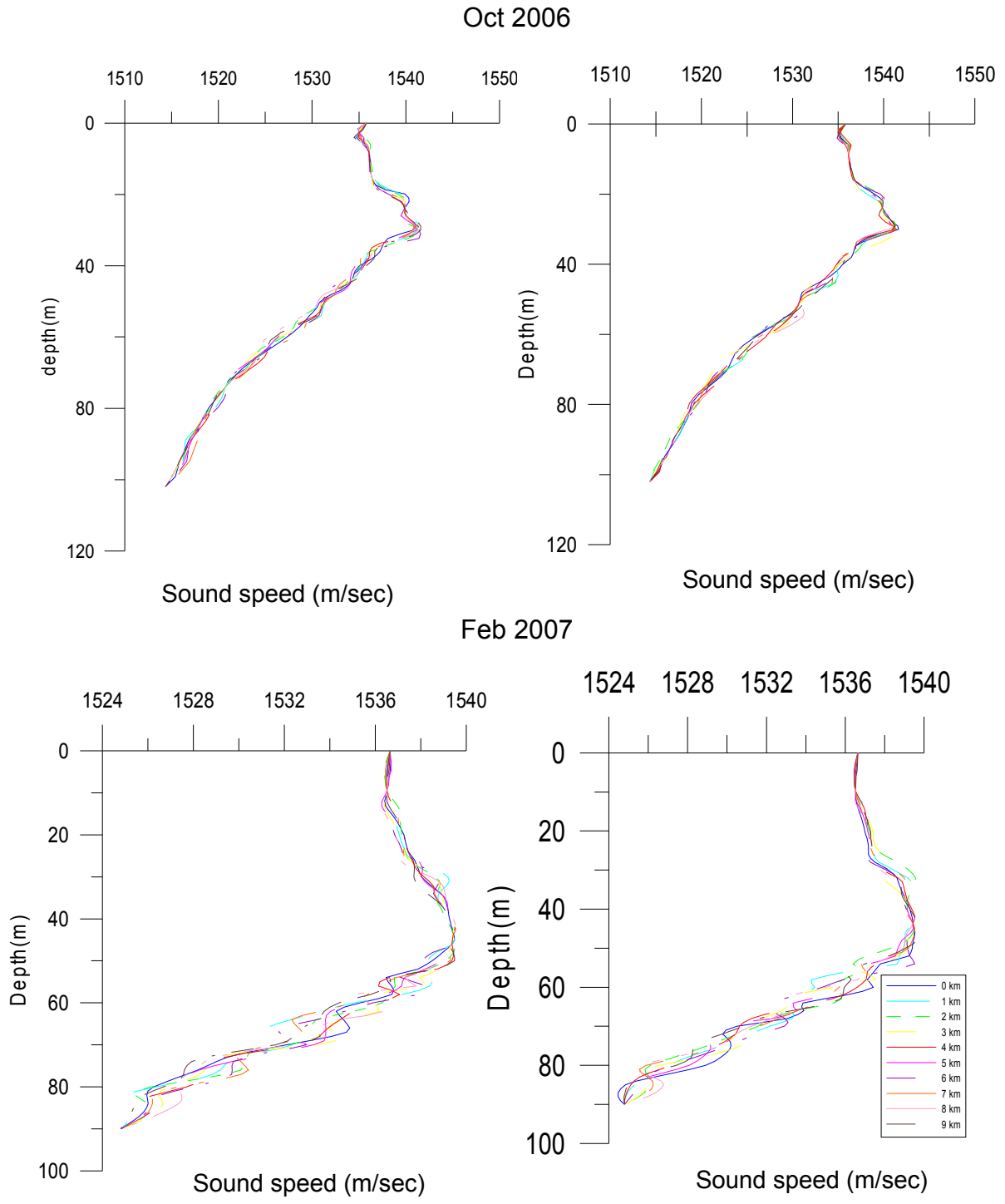
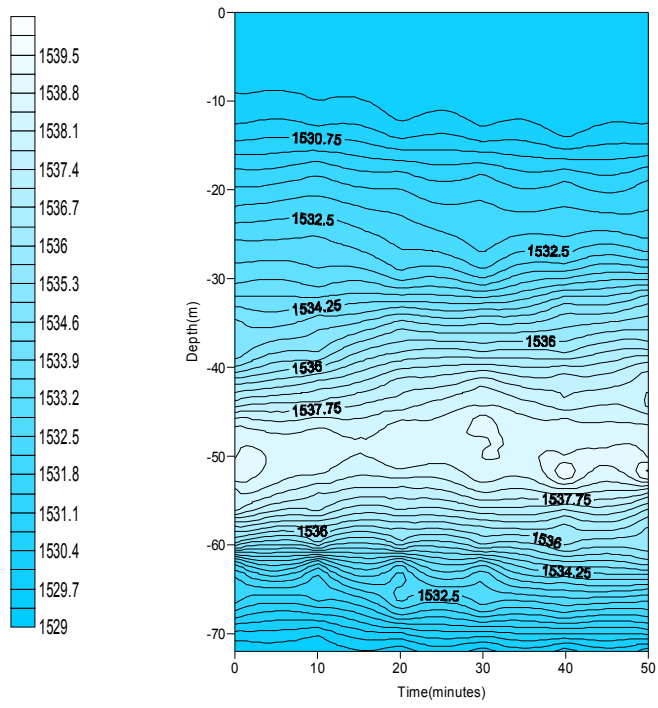
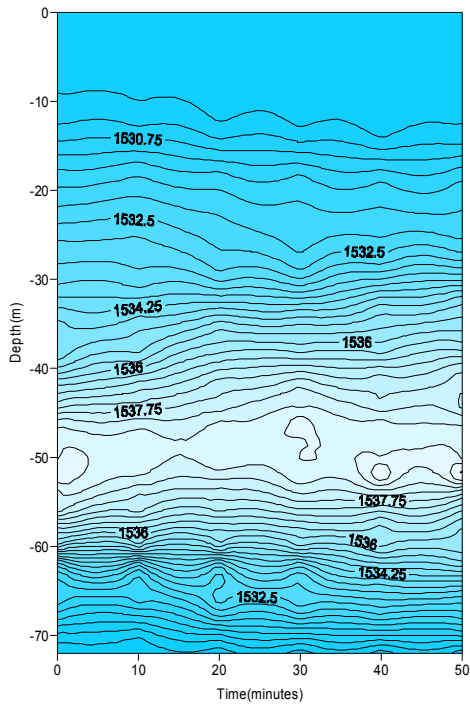
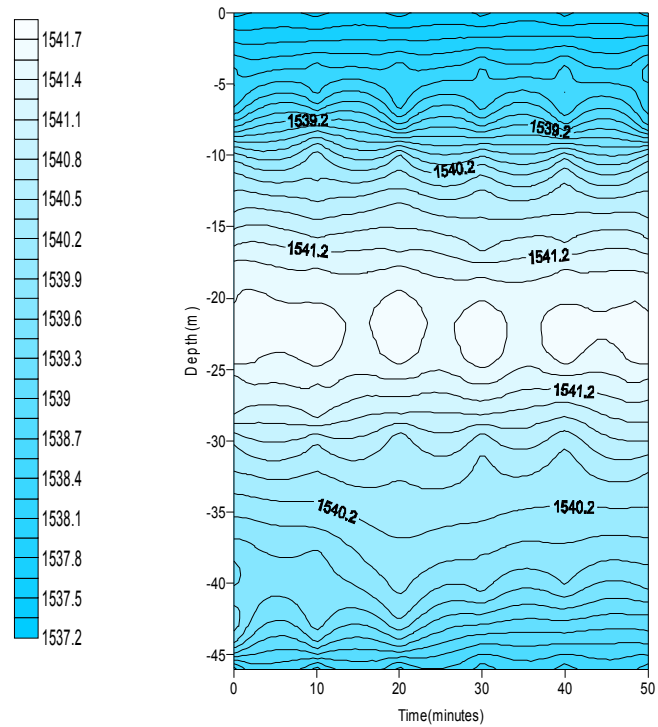
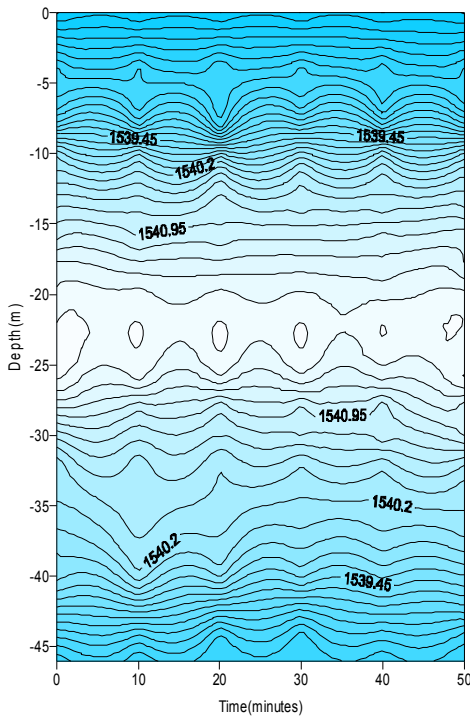


Figure 14: Sound velocity relations (a-single, b-double) in 9 km, 0.1 km apart off VSP & Bhimili

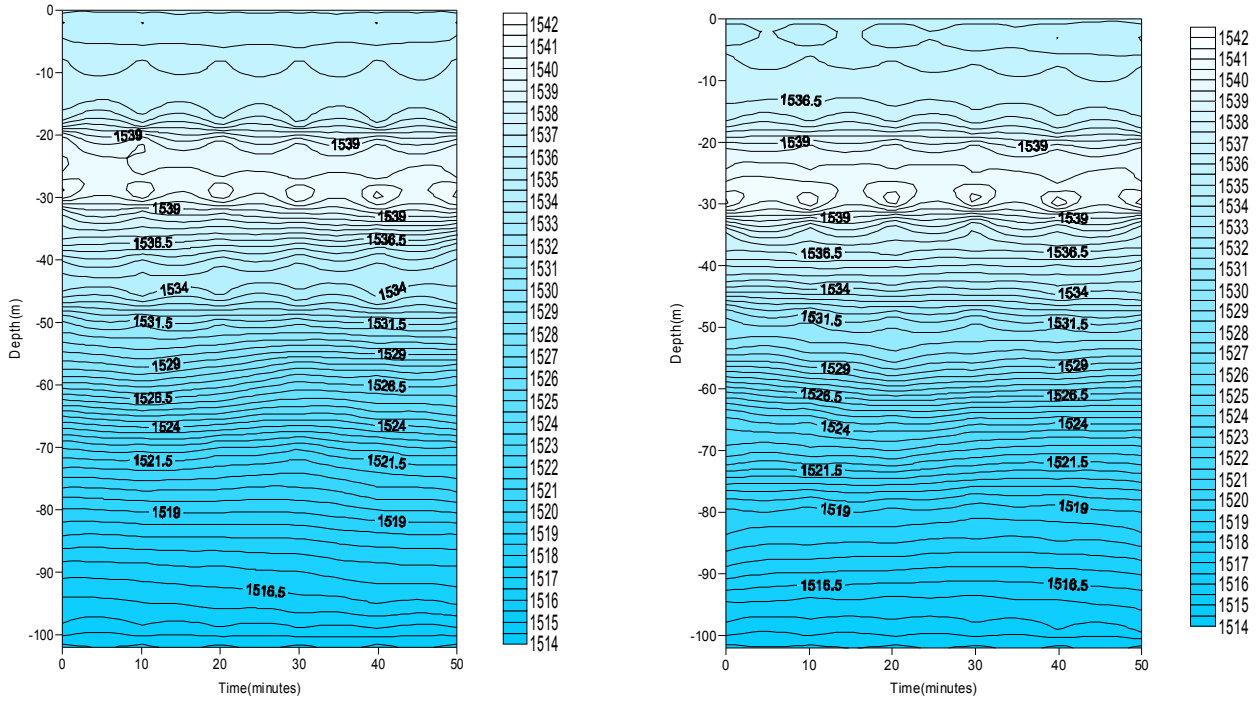
Jan 2005



Sep 2005



Oct 2006



Feb 2007

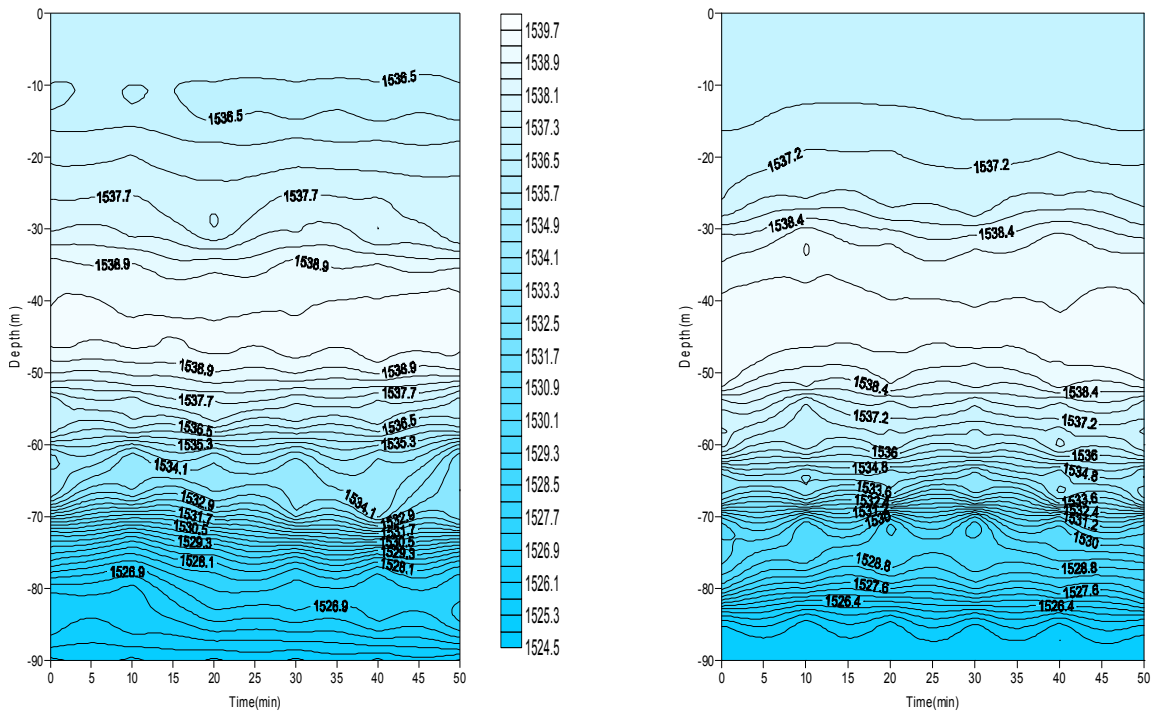
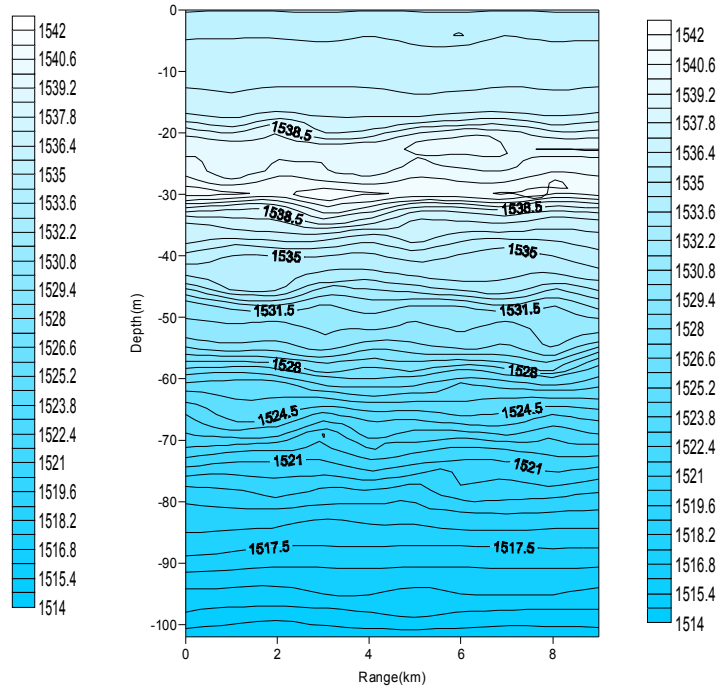
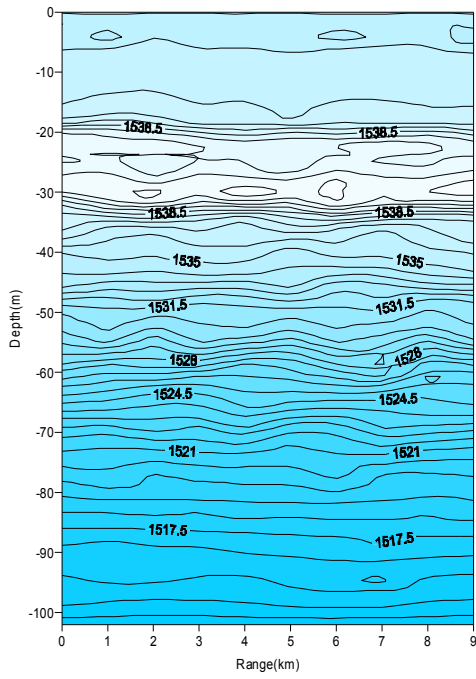


Figure 15: Temporal dependence of sound velocity distribution in the internal wave field (single & double realizations) off VSP & Bhimili

Oct 2006



Feb 2007

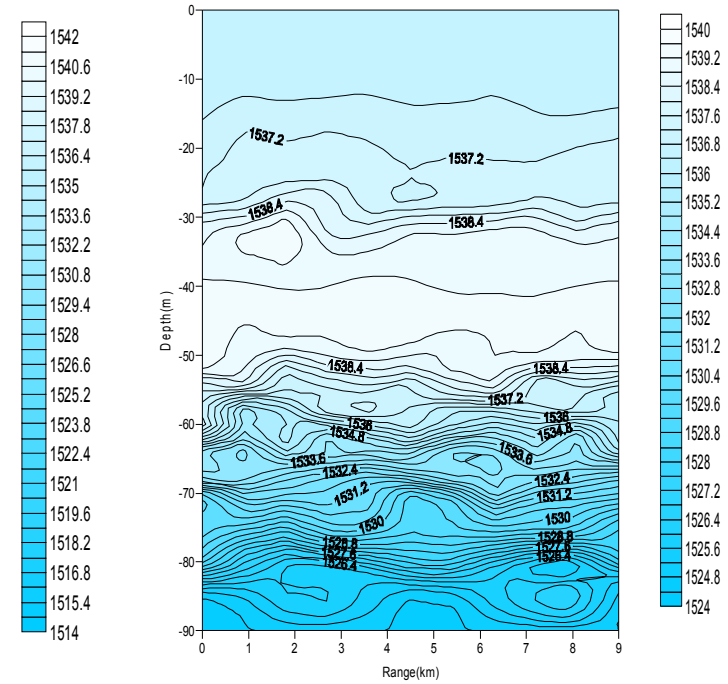
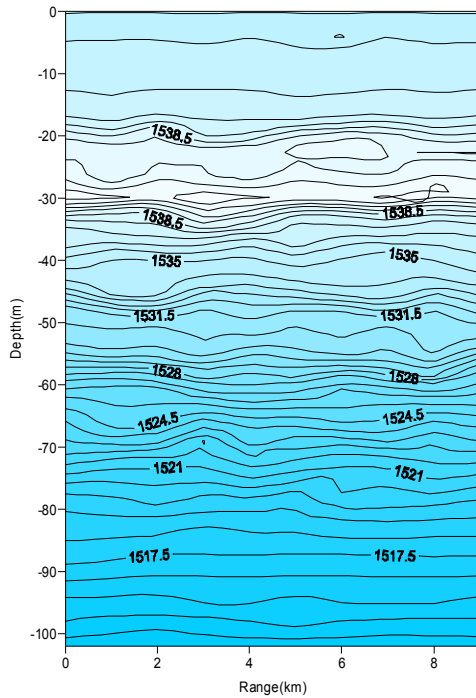
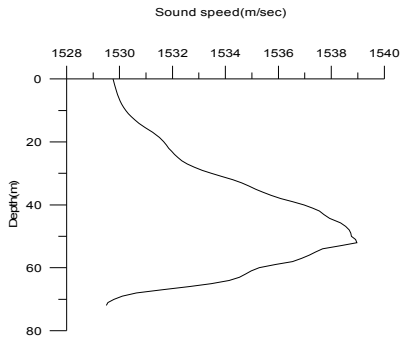


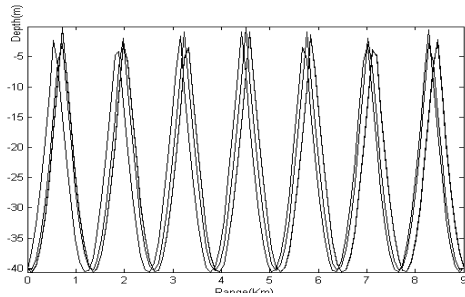
Figure 16: Spatial dependence of sound velocity distribution in the internal wave field (single & double realizations) off VSP & Bhimili

Sound Velocity (m/sec)



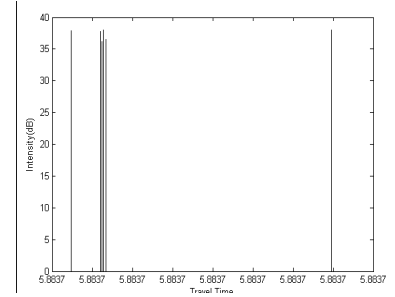
Mean of HF IW field

Eigen Rays



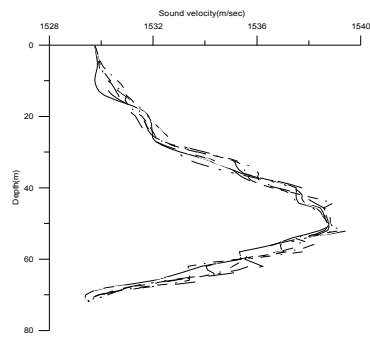
Range (km)

Intensity Jan 2005

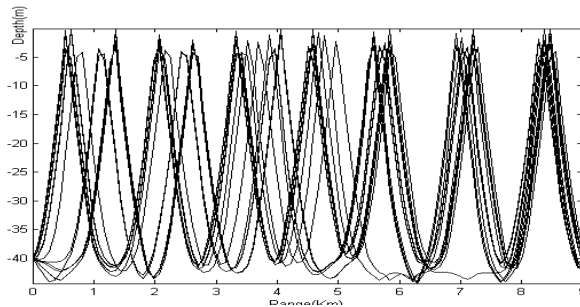


Travel Time (sec)

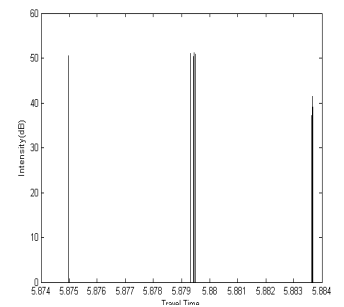
Jan 2005



Range –dependent of HF IW field

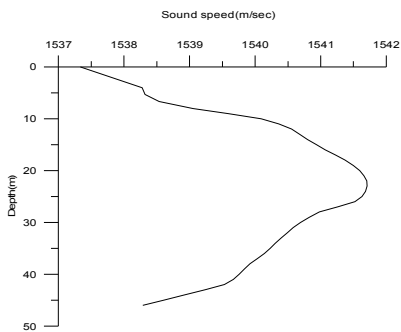


Range (km)

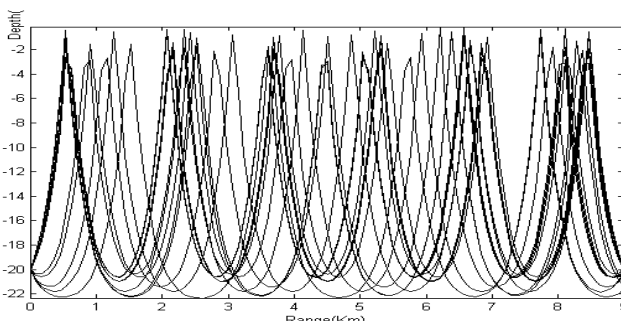


Travel Time (sec)

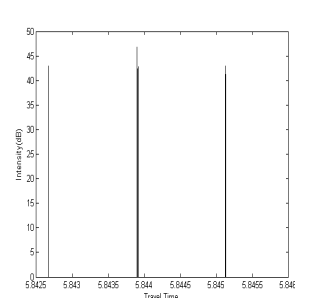
Sep 2005



Mean of HF IW field

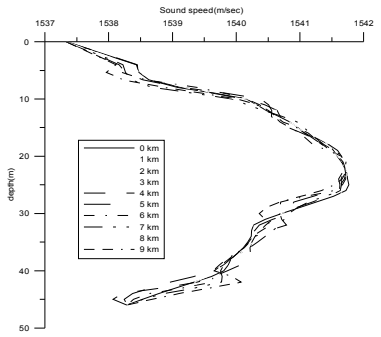


Range (km)



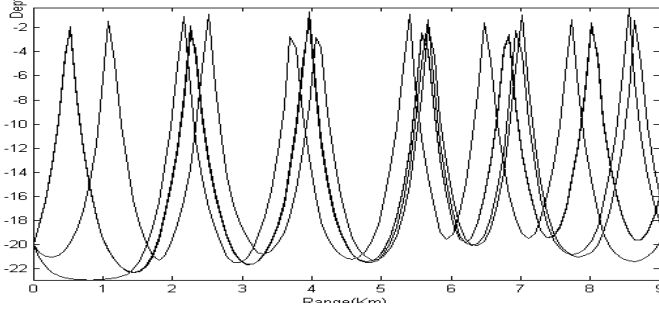
Travel Time (sec)

Sound Velocity



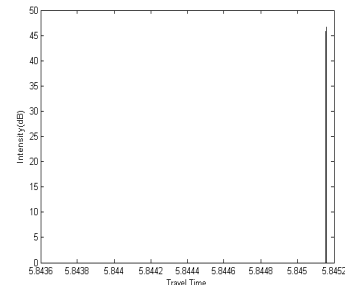
Range –dependent of HF IW field

Eigen Rays



Range (km)

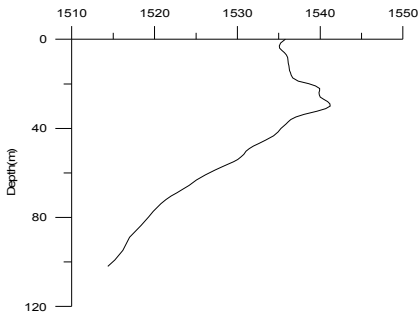
Intensity Sep 2005



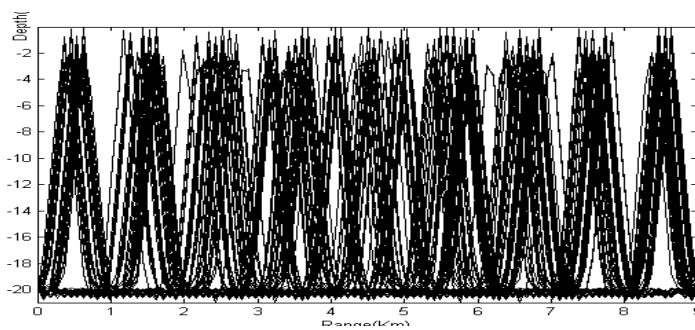
Travel Time (sec)

Oct 2006

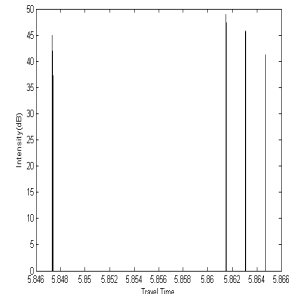
Sound speed(m/sec)



Mean of HF IW field



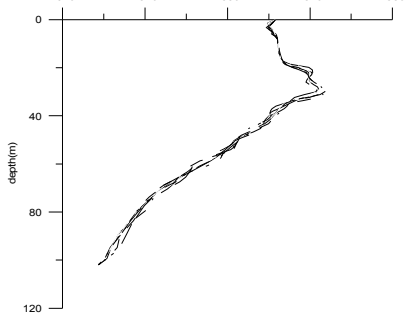
Range (km)



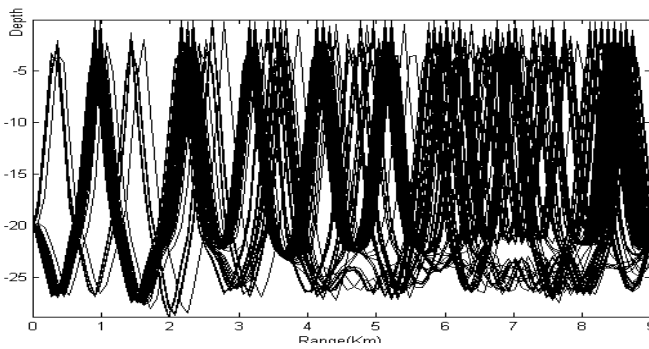
Travel Time (sec)

Oct 2006

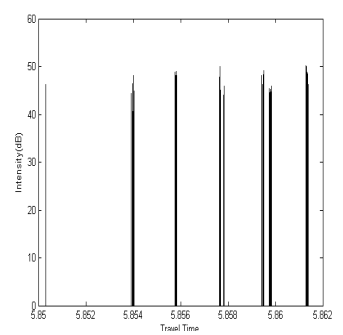
Sound velocity(m/sec)



Range –dependent of HF IW field

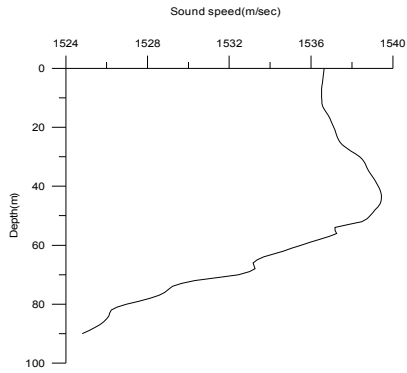


Range (km)

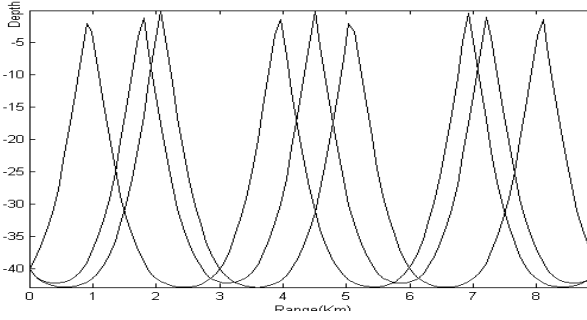


Travel Time (sec)

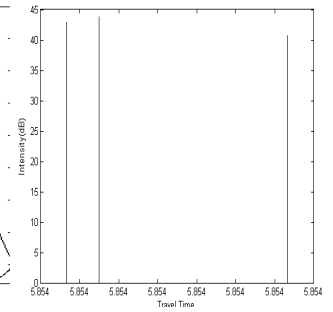
Sound Velocity



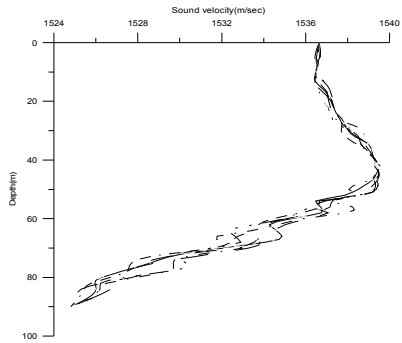
Eigen Rays



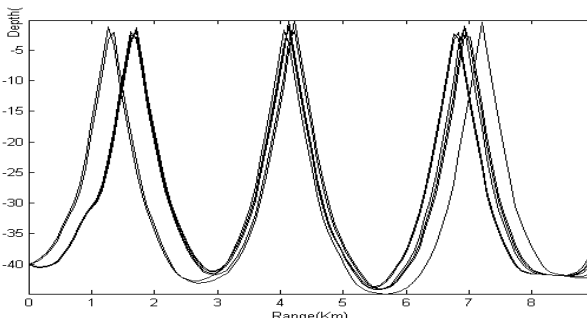
Intensity Feb 2007



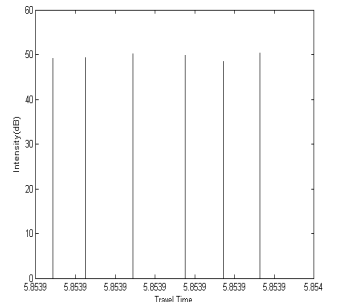
Mean of HF IW field



Range (km)



Travel Time (sec)



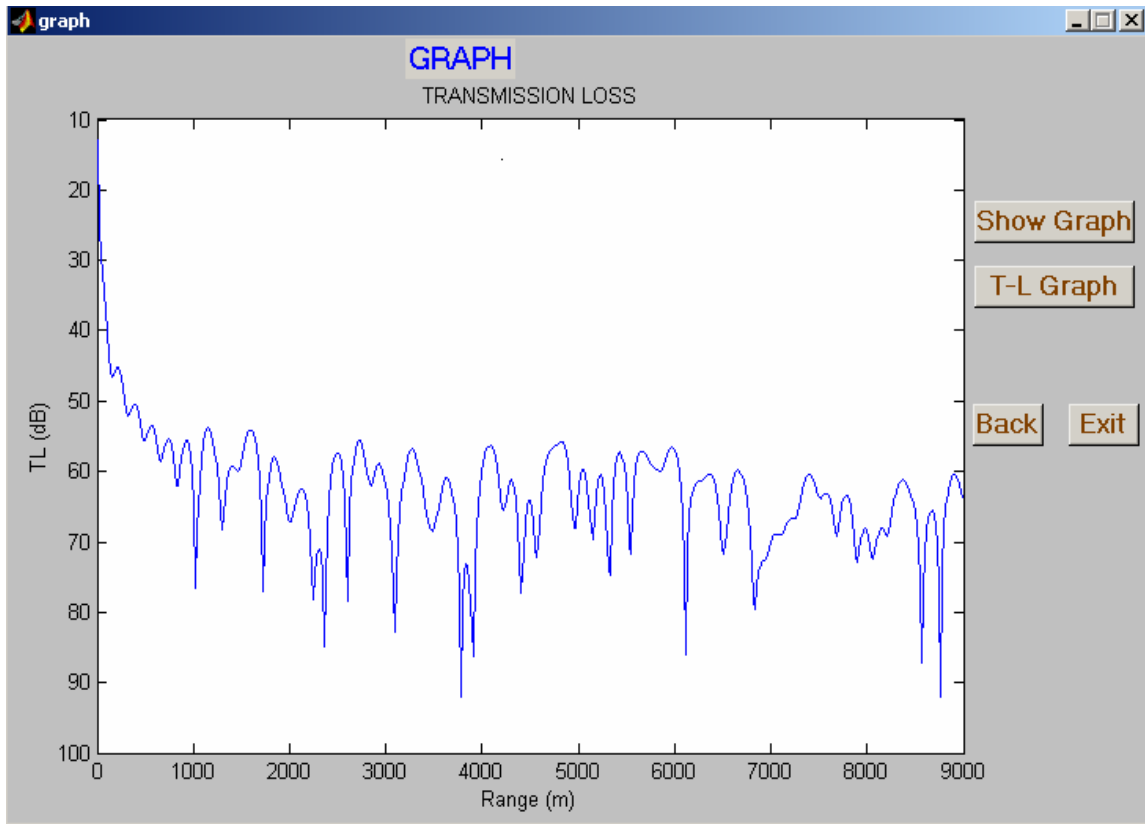
Feb 2007

Range -dependent of HF IW field

Range (km)

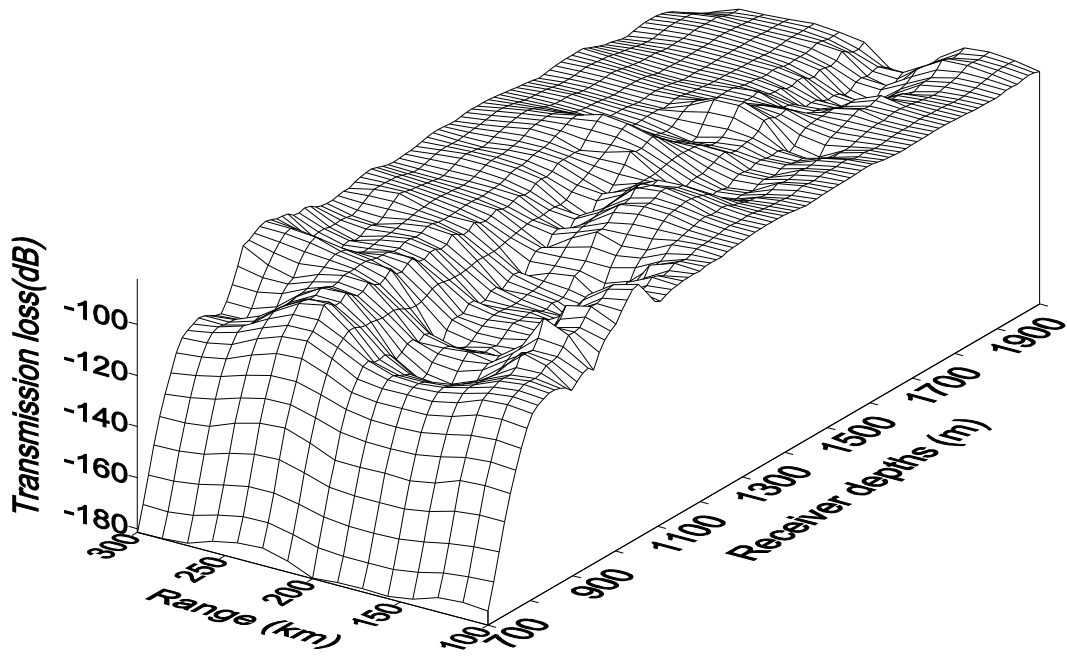
Travel Time (sec)

Figure 1.17: Ray paths



Source Depth(m) = 30.0 Frequency(Hz) = 2000.0
Receiver Depth(m) = 30.0 Range(Km) = 9.0
Sonic Depth(m) = 90.0

Figure 18: Transmission loss by Kracken model



Munk's canonical model profile :

$$\alpha = 250(m), \beta = 2490(m), Z_1 = 1490(m), C_1 = 1493.72(m/s)$$

$$B = 1.4148339(km), \varepsilon = 6.27009 \times 10^{-3}$$

α, β – upper and lower bounds of SOFAR channel B – stratification scale ε – perturbation coefficient

Z_1 – sound channel access C_1 – channel sound velocity

Figure 19: Transmission loss in 3-D form

Plate 1



Plate 2





Plates 1 and 2: Preparations for time-series data collection using CTD, Current Meters and thermister chain

Table 2: Internal Wave model run

Duration	f _{min} (cph)	f _{max} (cph)	No. of Freq.	No. of modes	Brunt vaisala freq(min) (cph)	Brunt vaisala freq.(max) (cph)
Jan05	0.5	8	750	40	0.0249	22.71
Sep05	0.5	1.5	100	40	0.0249	34.24
oct06	0.5	1.5	100	40	0.0249	24.57
Feb07	0.5	8.0	750	40	0.0251	17.592

Table 3: Internal wave characteristics off Visakhapatnam during Sep 2005
Internal wave velocity (c) – 0.029 km/hr

Depth (m)	Frequency (Low) (cph)	period (hrs)	Wavelength (km)	Frequency (high) (cph)	Period (hrs)	Wavelength (km)
10	0.32	3.125	0.090	4	0.25	0.00725
60	0.4	2.5	0.0725	3	0.33	0.00925
Average		2.81	0.081		0.29	0.0084

Table 4- Internal wave characteristics off Bhimili during Feb 2007
Internal wave velocity (c) – 0.042 km/hr

Depth (m)	Frequency (Low) (cph)	period (hrs)	Wavelength (km)	Frequency (high) (cph)	Period (hrs)	Wavelength (km)
0	0.04	24	1.008	7.5	0.133	0.0058
25	0.05	20	0.84	7.8	0.128	0.00538
50	0.02	50	2.1	7.8	0.128	0.00538
75	0.02	50	2.1	7.85	0.1273	0.00535
100	0.12	8.3	0.34	7.5	0.133	0.00558
Average		30	1.26		0.129	0.0054

Table 5-Internal wave characteristics of KG Basin

Duration	Velocity	Frequency (Low) (cph)	period (hrs)	Wavelength (km)	Frequency (high) (cph)	Period (hrs)	Wavelength (km)
Feb,04	0.0732	0.75	1.33	0.0973	1.5	0.667	0.048
Feb-Mar04	0.0700	0.75	1.33	0.093	1.5	0.667	0.046
Mar04	0.0600	0.75	1.33	0.79	1.5	0.667	0.041
Average		0.0600	1.33	0.79	1.5	0.667	0.041

Table 6- Acoustic Propogational Characteristics

Duration	MLD	Cut of Freq. (Hz)	No. of rays		Transmission laws (dB)		Anamoly (dB)	S-R configuration (m)
			I.W.	W.I.W	I.W.	W.I.W		
Jan05	62.5	379.47	20	7	54.128	57.539	3.41	40
Sep05	28	1265.5	3	17	62.578	93.272	30.694	20
Oct06	32.5	1011.9	200	103	52.233	42.255	9.98	20
Feb07	56.0	447.42	7	3	75.069	82.146	7.08	40

I.W — **In presence of Internal Waves**
W.I.W- **In absence of Internal Waves**
S-R – **Depth of source-receiver Configuration**

Table7: Acoustic ray parameters - January 2005
(Source depth = 40 m, Receiver depth = 40 m, Range = 9. km)

S.No	Θ_0 (deg)	θ_r (deg)	T(sec)	P^+	p^-	p_t^+	p_b^-	$P^+ + p^-$	$p_t^+ + p_b^-$	Σds	I/I_0
1	-0.01623	-0.00376	5.8794	6	6	6	0	12	6	9020.6	1.52E-10
2	-0.01623	-0.00376	5.8794	6	6	6	0	12	6	9020.6	1.52E-10
3	-0.01155	-0.04659	5.8793	6	6	6	0	12	6	9020.2	6.20E-11
4	-0.01151	0.015878	5.875	5	6	5	0	11	5	9016.9	8.04E-11
5	-0.00872	-0.02607	5.8794	6	6	6	0	12	6	9020.4	8.65E-11
6	-0.00837	0.003959	5.8794	6	7	6	0	13	6	9020.5	1.69E-10
7	-0.00812	-0.01945	5.8795	7	7	6	0	14	6	9019.8	6.84E-11
8	-0.00812	-0.01945	5.8795	7	7	6	0	14	6	9019.8	6.84E-11
9	-0.00704	-0.02825	5.8837	7	7	7	0	14	7	9022.6	4.53E-08
10	-0.00121	0.026829	5.8837	7	8	7	0	15	7	9022.3	3.00E-08
11	-0.00086	0.026825	5.8837	7	8	7	0	15	7	9022.3	1.19E-07
12	-0.00075	0.025965	5.8837	7	8	7	0	15	7	9022.3	1.19E-07
13	0.006097	0.027665	5.8837	7	7	7	0	14	7	9022.4	1.53E-08
14	0.006097	0.027665	5.8837	7	7	7	0	14	7	9022.4	1.53E-08
15	0.006936	0.027549	5.8837	7	7	7	0	14	7	9022.5	6.83E-08
16	0.012317	-0.03547	5.8836	7	6	7	0	13	7	9023.1	3.68E-08
17	0.012666	-0.03138	5.8836	7	6	7	0	13	7	9023	3.86E-08
18	0.012736	-0.03124	5.8836	7	6	7	0	13	7	9023	4.96E-09
19	0.015392	0.010902	5.8795	7	7	6	0	14	6	9020	5.32E-11
20	0.015392	0.010902	5.8795	7	7	6	0	14	6	9020	5.32E-11

θ_0 – ray launching angle at source, θ_r – ray angle at receiver, ds - ray path length, p^+ – number of upper turning points, p^- - number of lower turning points, p_t^+ - number of top bonks, p_b^- - number of bottom bonks, T - travel time, I/I_0 - acoustic intensity ratio

Table 8: Acoustic ray parameters - September 2005
(Source depth = 20 m, Receiver depth = 20 m, Range = 9. km)

S.No	$\Theta_0(\text{deg})$	$\theta_r(\text{deg})$	T(sec)	P^+	p^-	p_t^+	p_b^-	P^{++} p^-	p_t^{++} p_b^-	Σds	I/I_0
1	-0.01177	-0.00896	5.8439	5	5	5	0	10	5	9004.7	0
2	-0.01169	0.013238	5.8439	5	6	5	0	11	5	9004.7	0
3	-0.00981	0.019963	5.8439	5	6	5	0	11	5	9004.7	0
4	-0.00894	-0.00619	5.8451	6	6	6	0	12	6	9005.6	6.30E-11
5	0.015182	0.004127	5.8439	5	5	5	0	10	5	9004.8	2.38E-10
6	0.015356	0.021161	5.8451	6	6	6	0	12	6	9005.6	8.42E-10
7	0.015531	0.010514	5.8439	5	5	5	0	10	5	9004.8	0

θ_0 – ray launching angle at source, θ_r – ray angle at receiver, ds - ray path length, p^+ – number of upper turning points, p^- - number of lower turning points, p_t^+ - number of top bonks, p_b^- - number of bottom bonks, T - travel time, I/I_0 - acoustic intensity ratio

Table 9: Acoustic ray parameters - October 2006
(Source depth = 20 m, Receiver depth = 20 m, Range = 9. km)

S.No	$\Theta_0(\text{deg})$	$\theta_r(\text{deg})$	T(sec)	P^+	p^-	p_t^+	p_b^-	P^+ p^-	$p_t^+ p_b^-$	Σds	l/l_0
1	-0.01461	0.050471	5.8578	7	8	7	0	15	7	9011.6	6.28E-09
2	-0.01461	0.050471	5.8578	7	8	7	0	15	7	9011.6	6.28E-09
3	-0.01444	0.050913	5.8578	7	8	7	0	15	7	9011.6	6.42E-10
4	-0.01444	0.050913	5.8578	7	8	7	0	15	7	9011.6	6.42E-10
5	-0.01431	0.047856	5.8578	7	8	7	0	15	7	9011.6	1.56E-09
6	-0.01426	0.049529	5.8578	7	8	7	0	15	7	9011.5	1.09E-08
7	-0.01418	0.049653	5.8578	7	8	7	0	15	7	9011.5	2.19E-09
8	-0.01291	-0.0556	5.8558	8	8	6	0	16	6	9009.6	4.56E-10
9	-0.01282	-0.0653	5.8558	8	8	6	0	16	6	9009.5	1.72E-10
10	-0.01269	-0.04503	5.8558	8	8	6	0	16	6	9009.6	2.32E-10
11	-0.01269	-0.04503	5.8558	8	8	6	0	16	6	9009.6	2.32E-10
12	-0.01247	-0.04526	5.8558	8	8	6	0	16	6	9009.6	7.09E-10
13	-0.01234	0.009163	5.8558	7	8	6	0	15	6	9009.5	1.58E-10
14	-0.01225	-0.04123	5.8576	7	7	7	0	14	7	9010.9	2.73E-10
15	-0.01212	-0.0335	5.854	9	9	5	0	18	5	9008	8.39E-09
16	-0.01204	-0.03597	5.854	9	9	5	0	18	5	9007.9	2.53E-10
17	-0.01186	-0.01155	5.8577	7	7	7	0	14	7	9010.9	2.41E-09
18	-0.01177	-0.01228	5.854	9	9	5	0	18	5	9008	1.09E-09
19	-0.01169	-0.00507	5.8577	7	7	7	0	14	7	9010.9	2.40E-10
20	-0.01151	-0.03763	5.854	9	9	5	0	18	5	9007.9	2.92E-10
21	-0.01142	-0.02229	5.854	9	9	5	0	18	5	9008	2.45E-10
22	-0.01134	-0.04164	5.854	9	9	5	0	18	5	9007.9	7.34E-09
23	-0.01112	-0.02052	5.8595	8	8	8	0	16	8	9012.1	2.81E-09
24	-0.01112	-0.02052	5.8595	8	8	8	0	16	8	9012.1	2.81E-09
25	-0.01094	-0.04418	5.8558	8	8	6	0	16	6	9009.3	2.42E-10
26	-0.01073	-0.00641	5.8613	9	9	9	0	18	9	9013.2	1.87E-09
27	-0.01064	-0.01462	5.8595	8	8	8	0	16	8	9012.1	5.95E-09
28	-0.01046	-0.02421	5.8595	8	8	8	0	16	8	9012.1	3.19E-10
29	-0.01029	-0.01649	5.8595	8	8	8	0	16	8	9012.1	5.72E-10
30	-0.01025	-0.01634	5.8595	8	8	8	0	16	8	9012.1	2.11E-09
31	-0.01011	-0.0006	5.8613	9	9	9	0	18	9	9013.2	9.02E-11
32	-0.01011	-0.0006	5.8613	9	9	9	0	18	9	9013.2	9.02E-11
33	-0.00985	-0.01612	5.8595	8	8	8	0	16	8	9012.1	2.28E-10
34	-0.00981	0.016381	5.8577	7	8	7	0	15	7	9010.9	1.00E-10
35	-0.00955	0.014535	5.8613	9	10	9	0	19	9	9013.2	1.76E-10
36	-0.00955	0.014535	5.8613	9	10	9	0	19	9	9013.2	1.76E-10
37	-0.00946	-0.00553	5.8613	9	9	9	0	18	9	9013.2	1.11E-10
38	-0.00946	-0.00553	5.8613	9	9	9	0	18	9	9013.2	1.11E-10
39	-0.00924	0.039204	5.8613	9	10	9	0	19	9	9013.2	1.24E-09
40	-0.00924	0.039204	5.8613	9	10	9	0	19	9	9013.2	1.24E-09

41	-0.00872	0.004176	5.8613	9	10	9	0	19	9	9013.2	1.69E-10
42	-0.00872	0.004176	5.8613	9	10	9	0	19	9	9013.2	1.69E-10
43	-0.00806	0.030155	5.8613	9	10	9	0	19	9	9013.2	1.37E-09
44	-0.00806	0.030155	5.8613	9	10	9	0	19	9	9013.2	1.37E-09
45	-0.00793	0.040102	5.8613	9	10	9	0	19	9	9013.2	2.73E-10
46	-0.00793	0.040102	5.8613	9	10	9	0	19	9	9013.2	2.73E-10
47	-0.00762	0.039985	5.8613	9	10	9	0	19	9	9013.2	1.80E-10
48	-0.00762	0.039985	5.8613	9	10	9	0	19	9	9013.2	1.80E-10
49	-0.00754	0.035756	5.8613	9	10	9	0	19	9	9013.2	1.51E-09
50	-0.00754	0.035756	5.8613	9	10	9	0	19	9	9013.2	1.51E-09
51	-0.00745	0.040131	5.8613	9	10	9	0	19	9	9013.2	1.86E-10
52	-0.00736	0.020592	5.8613	9	10	9	0	19	9	9013.2	7.20E-10
53	-0.00723	0.028948	5.8613	9	10	9	0	19	9	9013.2	4.17E-10
54	-0.00723	0.028948	5.8613	9	10	9	0	19	9	9013.2	4.17E-10
55	-0.00714	0.042529	5.8613	9	10	9	0	19	9	9013.2	1.74E-09
56	-0.00706	0.028086	5.8613	9	10	9	0	19	9	9013.1	5.10E-10
57	-0.00666	0.040151	5.8613	9	10	9	0	19	9	9013.2	1.12E-09
58	-0.00666	0.040151	5.8613	9	10	9	0	19	9	9013.2	1.12E-09
59	-0.00653	0.040208	5.8613	9	10	9	0	19	9	9013.2	8.52E-10
60	-0.00644	0.041586	5.8613	9	10	9	0	19	9	9013.2	1.89E-10
61	-0.00636	0.040336	5.8613	9	10	9	0	19	9	9013.2	1.88E-10
62	-0.00636	0.040336	5.8613	9	10	9	0	19	9	9013.2	1.88E-10
63	-0.00618	0.045014	5.8613	9	10	9	0	19	9	9013.2	1.06E-09
64	-0.00614	0.032438	5.8613	9	10	9	0	19	9	9013.2	9.07E-10
65	-0.00579	0.019709	5.8613	9	10	9	0	19	9	9013.1	1.08E-09
66	-0.00579	0.019709	5.8613	9	10	9	0	19	9	9013.1	1.08E-09
67	-0.0057	0.010409	5.8613	9	10	9	0	19	9	9013.2	8.69E-10
68	-0.00566	0.039505	5.8613	9	10	9	0	19	9	9013.2	1.27E-09
69	-0.00566	0.039505	5.8613	9	10	9	0	19	9	9013.2	1.27E-09
70	-0.00553	0.008955	5.8613	9	10	9	0	19	9	9013.2	1.96E-10
71	-0.00544	0.040104	5.8613	9	10	9	0	19	9	9013.2	8.45E-10
72	-0.00544	0.040104	5.8613	9	10	9	0	19	9	9013.2	8.45E-10
73	-0.00505	0.018174	5.8613	9	10	9	0	19	9	9013.2	1.90E-10
74	-0.00496	0.046215	5.8614	9	10	9	0	19	9	9013.2	2.12E-10
75	-0.00487	0.040241	5.8613	9	10	9	0	19	9	9013.2	9.85E-10
76	-0.00487	0.040241	5.8613	9	10	9	0	19	9	9013.2	9.85E-10
77	-0.00448	0.026985	5.8613	9	10	9	0	19	9	9013.2	6.04E-10
78	-0.00448	0.026985	5.8613	9	10	9	0	19	9	9013.2	6.04E-10
79	-0.00435	0.039691	5.8613	9	10	9	0	19	9	9013.2	5.55E-09
80	-0.00426	0.0158	5.8613	9	10	9	0	19	9	9013.2	7.97E-10
81	-0.00408	0.01942	5.8613	9	10	9	0	19	9	9013.1	8.14E-10
82	-0.00408	0.01942	5.8613	9	10	9	0	19	9	9013.1	8.14E-10
83	-0.00382	0.020677	5.8613	9	10	9	0	19	9	9013.1	8.12E-10
84	-0.00378	0.044383	5.8613	9	10	9	0	19	9	9013.2	3.55E-09
85	-0.00369	0.027173	5.8613	9	10	9	0	19	9	9013.2	1.69E-09
86	-0.00365	0.039722	5.8613	9	10	9	0	19	9	9013.2	1.53E-09
87	-0.00356	0.035297	5.8613	9	10	9	0	19	9	9013.2	1.72E-09
88	-0.00356	0.035297	5.8613	9	10	9	0	19	9	9013.2	1.72E-09

89	-0.00291	0.037183	5.8613	9	10	9	0	19	9	9013.2	1.60E-09
90	-0.00291	0.037183	5.8613	9	10	9	0	19	9	9013.2	1.60E-09
91	-0.00225	0.041978	5.8613	9	10	9	0	19	9	9013.1	1.55E-09
92	-0.00225	0.041978	5.8613	9	10	9	0	19	9	9013.1	1.55E-09
93	-0.00208	0.040763	5.8613	9	10	9	0	19	9	9013.2	6.01E-10
94	-0.00203	0.033868	5.8613	9	10	9	0	19	9	9013.1	1.04E-09
95	-0.00194	0.039887	5.8613	9	10	9	0	19	9	9013.2	1.22E-09
96	-0.0019	0.00975	5.8613	9	10	9	0	19	9	9013.1	5.27E-10
97	-0.00181	0.039826	5.8613	9	10	9	0	19	9	9013.2	1.63E-09
98	-0.00177	0.0147	5.8613	9	10	9	0	19	9	9013.2	1.81E-10
99	-0.00164	0.038159	5.8613	9	10	9	0	19	9	9013.2	1.03E-10
100	-0.00164	0.038159	5.8613	9	10	9	0	19	9	9013.2	1.03E-10
101	-0.00024	0.024928	5.8613	9	10	9	0	19	9	9013.1	5.57E-10
102	-0.0002	0.050802	5.8614	9	10	9	0	19	9	9013.2	7.33E-10
103	0.002075	0.038291	5.8613	10	10	9	0	20	9	9013.1	8.30E-10
104	0.002075	0.038291	5.8613	10	10	9	0	20	9	9013.1	8.30E-10
105	0.002425	0.02419	5.8613	10	10	9	0	20	9	9013.1	4.64E-10
106	0.002425	0.02419	5.8613	10	10	9	0	20	9	9013.1	4.64E-10
107	0.002643	0.032266	5.8613	10	10	9	0	20	9	9013.1	4.78E-10
108	0.002643	0.032266	5.8613	10	10	9	0	20	9	9013.1	4.78E-10
109	0.004303	0.041901	5.8613	10	10	9	0	20	9	9013.2	1.11E-09
110	0.004347	0.030012	5.8613	10	10	9	0	20	9	9013.1	6.25E-10
111	0.004915	0.037989	5.8613	10	10	9	0	20	9	9013.2	2.28E-09
112	0.004915	0.037989	5.8613	10	10	9	0	20	9	9013.2	2.28E-09
113	0.005221	0.02414	5.8613	10	10	9	0	20	9	9013.2	2.47E-10
114	0.005221	0.02414	5.8613	10	10	9	0	20	9	9013.2	2.47E-10
115	0.005658	0.023889	5.8613	10	10	9	0	20	9	9013.2	9.23E-11
116	0.005745	0.047296	5.8614	10	10	9	0	20	9	9013.2	1.99E-10
117	0.005832	0.039712	5.8613	10	10	9	0	20	9	9013.2	3.17E-10
118	0.005876	0.039678	5.8613	10	10	9	0	20	9	9013.2	1.45E-09
119	0.005963	0.039454	5.8613	10	10	9	0	20	9	9013.2	3.87E-09
120	0.006051	0.039493	5.8613	10	10	9	0	20	9	9013.2	2.76E-09
121	0.006269	0.040085	5.8613	10	10	9	0	20	9	9013.2	1.25E-09
122	0.006269	0.040085	5.8613	10	10	9	0	20	9	9013.2	1.25E-09
123	0.0064	0.022138	5.8613	10	10	9	0	20	9	9013.2	9.54E-10
124	0.006488	0.002989	5.8613	10	10	9	0	20	9	9013.2	1.17E-09
125	0.006575	0.009052	5.8613	10	10	9	0	20	9	9013.2	5.71E-10
126	0.006619	0.046774	5.8614	10	10	9	0	20	9	9013.2	1.79E-09
127	0.006619	0.046774	5.8614	10	10	9	0	20	9	9013.2	1.79E-09
128	0.006662	0.012757	5.8613	10	10	9	0	20	9	9013.2	2.85E-09
129	0.00675	0.050407	5.8614	10	10	9	0	20	9	9013.2	1.21E-09
130	0.006837	0.053203	5.8614	10	10	9	0	20	9	9013.2	2.20E-10
131	0.006925	0.014392	5.8613	10	10	9	0	20	9	9013.2	2.04E-10
132	0.006925	0.014392	5.8613	10	10	9	0	20	9	9013.2	2.04E-10
133	0.007012	0.000631	5.8613	10	10	9	0	20	9	9013.2	9.29E-11
134	0.007012	0.000631	5.8613	10	10	9	0	20	9	9013.2	9.29E-11
135	0.007099	0.039036	5.8613	10	10	9	0	20	9	9013.2	9.62E-11
136	0.007099	0.039036	5.8613	10	10	9	0	20	9	9013.2	9.62E-11

137	0.007274	0.054391	5.8595	9	9	8	0	18	8	9012	1.95E-10
138	0.007318	-0.00146	5.8613	10	9	9	0	19	9	9013.2	1.21E-10
139	0.007405	-0.00501	5.8613	10	9	9	0	19	9	9013.2	2.31E-10
140	0.007405	-0.00501	5.8613	10	9	9	0	19	9	9013.2	2.31E-10
141	0.007536	-0.01328	5.8613	10	9	9	0	19	9	9013.2	7.28E-10
142	0.007536	-0.01328	5.8613	10	9	9	0	19	9	9013.2	7.28E-10
143	0.008192	-0.00248	5.8613	10	9	9	0	19	9	9013.2	9.08E-11
144	0.008192	-0.00248	5.8613	10	9	9	0	19	9	9013.2	9.08E-11
145	0.008541	-0.0128	5.8613	10	9	9	0	19	9	9013.2	1.80E-10
146	0.008541	-0.0128	5.8613	10	9	9	0	19	9	9013.2	1.80E-10
147	0.008628	-0.00199	5.8613	10	9	9	0	19	9	9013.2	1.13E-10
148	0.008628	-0.00199	5.8613	10	9	9	0	19	9	9013.2	1.13E-10
149	0.008716	0.001417	5.8613	10	10	9	0	20	9	9013.2	3.83E-09
150	0.008716	0.001417	5.8613	10	10	9	0	20	9	9013.2	3.83E-09
151	0.008803	-0.01346	5.8613	10	9	9	0	19	9	9013.2	1.82E-10
152	0.008847	0.043706	5.854	10	10	5	0	20	5	9007.6	5.35E-10
153	0.008934	0.003693	5.8613	10	10	9	0	20	9	9013.2	2.06E-10
154	0.008934	0.003693	5.8613	10	10	9	0	20	9	9013.2	2.06E-10
155	0.009022	-0.01899	5.8613	10	9	9	0	19	9	9013.2	4.10E-09
156	0.009109	0.000371	5.8613	10	10	9	0	20	9	9013.2	9.51E-09
157	0.009196	0.006641	5.8613	10	10	9	0	20	9	9013.2	2.08E-10
158	0.009371	0.043002	5.854	10	10	5	0	20	5	9007.6	6.25E-10
159	0.009502	0.059948	5.854	10	10	5	0	20	5	9007.7	2.60E-10
160	0.009677	-0.05602	5.8594	9	8	8	0	17	8	9012.1	2.41E-10
161	0.009677	-0.05602	5.8594	9	8	8	0	17	8	9012.1	2.41E-10
162	0.009895	-0.01334	5.8595	9	8	8	0	17	8	9012.1	1.09E-09
163	0.010026	0.043792	5.854	10	10	5	0	20	5	9007.6	7.75E-10
164	0.010157	0.000137	5.8577	8	8	7	0	16	7	9010.9	1.91E-10
165	0.010288	-0.02033	5.8595	9	8	8	0	17	8	9012.1	3.91E-10
166	0.010332	-0.04099	5.854	11	10	5	0	21	5	9007.8	4.46E-09
167	0.01042	-0.01571	5.8595	9	8	8	0	17	8	9012.1	1.74E-09
168	0.010551	0.003759	5.8613	10	10	9	0	20	9	9013.2	2.04E-10
169	0.010682	-0.04339	5.8595	9	8	8	0	17	8	9012.1	5.45E-10
170	0.010682	-0.04339	5.8595	9	8	8	0	17	8	9012.1	5.45E-10
171	0.010769	0.031834	5.8539	10	10	5	0	20	5	9007.6	1.35E-09
172	0.010813	0.033533	5.8577	8	8	7	0	16	7	9011	9.62E-10
173	0.011075	-0.01521	5.8595	9	8	8	0	17	8	9012.1	2.16E-10
174	0.011206	0.054132	5.8503	11	11	3	0	22	3	9004.8	5.77E-10
175	0.011293	0.003204	5.8558	9	9	6	0	18	6	9009.3	1.06E-09
176	0.011381	-0.01736	5.8595	9	8	8	0	17	8	9012.1	7.95E-10
177	0.011512	-0.01361	5.8595	9	8	8	0	17	8	9012.1	1.48E-10
178	0.011555	-0.03222	5.8595	9	8	8	0	17	8	9012.1	5.77E-10
179	0.011599	0.057704	5.854	9	9	5	0	18	5	9007.6	4.35E-10
180	0.011643	-0.00409	5.8613	10	9	9	0	19	9	9013.2	3.76E-10
181	0.011905	0.003741	5.8613	10	10	9	0	20	9	9013.2	1.64E-10
182	0.011905	0.003741	5.8613	10	10	9	0	20	9	9013.2	1.64E-10
183	0.012123	0.039062	5.8613	10	10	9	0	20	9	9013.2	1.82E-10
184	0.012123	0.039062	5.8613	10	10	9	0	20	9	9013.2	1.82E-10

185	0.012254	0.040405	5.8613	10	10	9	0	20	9	9013.2	1.71E-10
186	0.012386	0.058665	5.8614	10	10	9	0	20	9	9013.2	5.86E-10
187	0.012386	0.058665	5.8614	10	10	9	0	20	9	9013.2	5.86E-10
188	0.012517	0.049319	5.8597	8	8	8	0	16	8	9013.6	8.35E-10
189	0.014046	0.051658	5.8598	8	8	8	0	16	8	9013.5	1.07E-09
190	0.014177	0.052789	5.8598	8	8	8	0	16	8	9013.5	2.42E-09
191	0.014308	0.053521	5.8598	8	8	8	0	16	8	9013.5	2.53E-09
192	0.014395	0.051858	5.8598	8	8	8	0	16	8	9013.5	9.18E-10
193	0.014395	0.051858	5.8598	8	8	8	0	16	8	9013.5	9.18E-10
194	0.014614	0.058318	5.8598	8	8	8	0	16	8	9013.6	1.12E-09
195	0.014657	0.063186	5.8598	8	8	8	0	16	8	9013.6	6.54E-10
196	0.016012	0.061928	5.8598	8	8	8	0	16	8	9013.6	7.62E-10
197	0.016055	0.048381	5.8598	8	8	8	0	16	8	9013.5	3.37E-09
198	0.016667	0.037856	5.8597	8	8	8	0	16	8	9013.4	3.05E-09
199	0.017366	0.049496	5.8598	8	8	8	0	16	8	9013.5	1.11E-09
200	0.017366	0.049496	5.8598	8	8	8	0	16	8	9013.5	1.11E-09

θ_0 – ray launching angle at source, θ_r – ray angle at receiver, d_s - ray path length, p^+ – number of upper turning points, p^- - number of lower turning points, p_t^+ - number of top bonks, p_b^- - number of bottom bonks, T - travel time, I/I_0 - acoustic intensity ratio

Table 10: Acoustic ray parameters
(Source depth = 40 m, Receiver depth = 40 m, Range = 9. km)

S.No	Θ_0 (deg)	θ_r (deg)	T(sec)	P^+	p^-	p_t^+	p_b^-	P^+ p^-	p_t^+ p_b^-	Σds	I/I_0
1	-0.00496	0.019366	5.8539	3	4	3	0	7	3	9005.7	9.31E-11
2	-0.00482	0.026644	5.8539	3	4	3	0	7	3	9005.8	8.33E-11
3	-0.00462	0.010451	5.8539	3	4	3	0	7	3	9005.7	1.44E-10
4	-0.00449	0.022436	5.8539	3	4	3	0	7	3	9005.8	1.12E-10
5	0.002011	0.001218	5.8539	3	3	3	0	6	3	9005.8	1.33E-10
6	0.002011	0.001218	5.8539	3	3	3	0	6	3	9005.8	1.33E-10
7	0.002988	0.021914	5.8539	3	3	3	0	6	3	9005.9	1.88E-10

θ_0 – ray launching angle at source, θ_r – ray angle at receiver, ds - ray path length, p^+ – number of upper turning points, p^- - number of lower turning points, p_t^+ - number of top bonks, p_b^- - number of bottom bonks, T - travel time, I/I_0 - acoustic intensity ratio